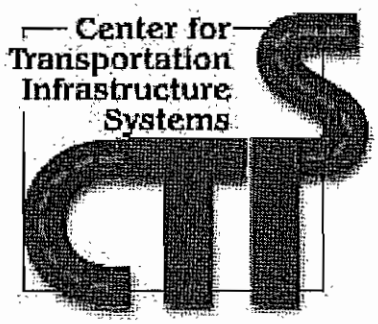

Evaluation of Binder Tests for Identifying Rutting and Cracking Potential of Modified Asphalt Binders

Research Report 0-4824-1
Project Number 0-4824

Conducted for

Texas Department of Transportation
P.O. Box 5080
Austin, Texas 78763

February 2007

Center for Transportation Infrastructure Systems
The University of Texas at El Paso
El Paso, Texas 79968
(915) 747-6925

[This page replaces an intentionally blank page in the original document. --CTR Library digitization project]

TECHNICAL REPORT STANDARD TITLE PAGE

1. Report No. FHWA/TX-07/0-4824-1	2. Government Accession No.	3. Recipient's Catalog No.
4. Title and Subtitle Evaluation of Binder Tests for Identifying Rutting and Cracking Potential of Modified Asphalt Binders		**5. Report Date** February 2007 **6. Performing Organization Code**
7. Author(s) Gina M. Hrdlicka, BS Vivek Tandon, PhD, PE Jorge Prozzi, PhD Andre Smit, PhD Yetkin Yildrim, PhD		**8. Performing Organization Report No.** 0-4824-1
9. Performing Organization Name and Address Center for Transportation Infrastructure Systems The University of Texas at El Paso El Paso, Texas 79968-0516		**10. Work Unit No.** **11. Contract or Grant No.** 0-4824
12. Sponsoring Agency Name and Address Texas Department of Transportation Research and Technology Implementation Office P.O. Box 5080 Austin, Texas 78763		**13. Type of Report and Period Covered** Technical Report: September 03 thru July 06 **14. Sponsoring Agency Code**

15. Supplementary Notes
Research performed in cooperation with the Texas Department of Transportation and the Federal Highway Administration.
Project title: Guidelines for Selecting Asphalt Mixtures and Evaluation of Polymer-Modified Mixes

16. Abstract
To minimize premature failures, the Strategic Highway Research Program (SHRP) proposed binder tests that can identify poorly performing binders. To meet new performance grade specifications, a modifier is typically added to the binder. Occasionally, state highway agencies specify a particular modifier type and modifier content to be included in the binder. However, the specified asphalt binder or tests do not necessarily identify the presence of modifiers. Therefore, the focus of the research was to identify a suitable binder test that can detect the presence of modifier and rutting and cracking potential of hot mix asphalt concrete. In addition, the purpose of the study was to identify whether a particular modifier is better in comparison to the other available modifiers or they provide the similar performances.

17. Key Words	18. Distribution Statement
HWTD, Fatigue, Rutting, Repeated Creep, Frequency Sweep, Binder, Modifier.	No restrictions. This document is available to the public through the National Technical Information Service, Spring field, Virginia 22161, www.ntis.gov

19. Security Classif. (of this report)	20. Security Classif. (of this page)	21. No. of Pages	22. Price
Unclassified	Unclassified	82	

[This page replaces an intentionally blank page in the original document. --CTR Library digitization project]

Evaluation of Binder Tests for Identifying Rutting and Cracking Potential of Modified Asphalt Binders

By

Gina M. Hrdlicka, BS
Vivek Tandon, PhD, PE
Jorge Prozzi, PhD
Andre Smit, PhD
Yetkin Yildrim, PhD

Report Number 0-4824-1
Project Number 0-4824

Project Title: **Guidelines for Selecting Asphalt Mixtures and Evaluation of Polymer-Modified Mixes**

Performed in cooperation with the

Texas Department of Transportation and the Federal Highway Administration

The Center for Transportation Infrastructure Systems
The University of Texas at El Paso
El Paso, Texas 79968-0516
February 2007

Disclaimer:

The contents of this report reflect the view of the authors, who are responsible for the facts and the accuracy of the data presented herein. The contents do not necessarily reflect the official views or policies of the Texas Department of Transportation or the Federal Highway Administration. This report does not constitute a standard, specification, or regulation.

NOT INTENDED FOR CONSTRUCTION, BIDDING, OR PERMIT PURPOSES

Gina M. Hrdlicka, BS
Vivek Tandon, PhD, PE (88219)
Jorge Prozzi, PhD
Andre Smit, PhD
Yetkin Yildrim, PhD

ACKNOWLEDGEMENTS

The successful progress of this project could not have happened without the valuable assistance from a number of TxDOT personnel. The authors acknowledge Dr. Magdy Mikhail (PD) and Mr. Elias Rmeili (PC) for facilitating collaboration with TxDOT Districts. They also provided valuable guidance and input. In addition, the authors would like to acknowledge Ms. Valeria Lopez, Mr. Edgar Gurerro and Mr. Issac Puentes, for their assistance in performing tests.

ABSTRACT

In recent decades, the Strategic Highway Research Program (SHRP) recommended new performance based specifications for asphalt binders, known as Performance Grade (PG) Specifications which suggest performing tests at the service temperature rather than a set temperature. To meet these new PG-specifications, manufacturers either altered manufacturing practices such as air blown asphalt, or added modifiers such as polymers. In general, the addition of modifiers improved the performance of hot mix asphalt concrete (HMAC), while the air blown or acid modified asphalt decreased the durability of the mixes.

The new performance tests are unable to differentiate between polymer modified asphalts and acid modified asphalt. To overcome this problem, the elastic recovery test has been specified by the highway agencies because it can differentiate between an asphalt binder consisting of modifier and acid modified asphalt binders. However, discussions with asphalt producers identified that the asphalt modified with Styrene Butadiene Rubber (SBR) does not pass elastic recovery tests but performs well in the field. In addition, the test does not provide any fundamental property of asphalt binder.

Recently, the repeated creep test has been proposed by the Federal Highway Administration (FHWA) to measure the fundamental properties of asphalt binders and can be used to identify the presence of modifiers. Therefore, the objective of this study was to evaluate the capability of the repeated creep test in detecting the presence of modifiers.

Typically, rutting is one of the major causes of premature failure of HMAC, especially within Texas. To identify rutting potential of HMAC, the Hamburg Wheel Tracking Device (HWTD) test was specified by the Texas Department of Transportation (TxDOT). If HWTD test results identify a mix to be rut susceptible, the test results do not necessarily indicate whether the mix design and/or asphalt binder is the major factor responsible for rutting potential. It may be possible for the repeated creep test results to identify the rutting potential, thus identifying whether or not the asphalt binder is the contributing factor. Therefore, another objective of this study was to identify rutting potential of a mix consisting of rut prone asphalt binder using repeated creep tests. If a correlation can be established between the properties of the asphalt binders used in the HMAC and the rutting potential displayed in laboratory testing, the premature failure can be minimized. It is expected that the addition of modifiers can significantly increase the binder stiffness at lower temperatures. To evaluate the increase in fatigue resistance and to make sure that the mixes are not brittle, the cracking potential of binder consisting of modifiers needs to be evaluated as well.

To perform this study, two mix designs used by TxDOT, Type-D and Coarse Matrix High Binder (CMHB-C), were selected. The Type-D mix was obtained

from the Austin District and the CMHB-C from the Bryan District. Both of the chosen mixes have shown success in the field and have recently been placed using modifiers. The modifiers assessed in this study include, Styrene-Butadiene-Styrene (SBS), Styrene-Butadiene-Rubber (SBR), Tire Rubber (TR), and Elvaloy. Since the mix types are well performing and mix designs are the same, the major factor contributing towards rutting of HMAC can be traced to the asphalt binder, which is the only component that is altered between the mixes.

The test results suggested that the presence of modifiers can be detected using repeated creep tests and can be used to identify the rutting potential of HMAC. In addition, a relationship between mix types and accumulated strains (from repeated creep tests) has been proposed. The developed relationships were further validated using PREES Procedure. Results suggest that repeated creep tests have the likelihood of identifying the rutting potential of HMAC. The test results also suggest that the modifiers improve performance but whether or not a specific modifier is better than another cannot be identified.

TABLE OF CONTENTS

LIST OF FIGURES

LIST OF TABLES

CHAPTER 1 INTRODUCTION

1.1 INTRODUCTION

In recent decades, the Strategic Highway Research Program (SHRP) suggested new performance based specifications for asphalt binders to be used in the hot mix asphalt concrete (HMAC). These new specifications, known as Performance Grade (PG) Specifications, suggest performing tests at the service temperature rather than a set temperature, as outlined in the previous specifications. To meet these new PG-specifications, manufacturers either altered manufacturing practices such as air blown asphalt or added modifiers such as polymers (King et al., 1999). In general, the addition of modifiers improved the performance of HMAC while the air blown asphalt or acid modifications decreased the durability of the mixes (King et al., 1999).

Typically, the new performance tests are unable to differentiate between polymer modified asphalts and acid modified asphalt (Anderson et. al., 2002). To make sure that manufacturers provided modified asphalt binder, state highway agencies started specifying type and percentage of modifier. Occasionally, the percent and type of modifier specified is strictly governed by anecdotal information rather than actual performance evaluations. In recent years, the elastic recovery test (ASTM D 6084 and Tex-539-C) has been proposed as the test that can differentiate between asphalt binders consisting of modifier and acid modified asphalt binders. However, discussions with the asphalt producers identified that the asphalt modified with Styrene Butadiene Rubber (SBR) does not pass elastic recovery test but performs well in the field. The test evaluates elasticity of the modified asphalt and may not be suitable for asphalt modified with non-elastomer type polymers. In addition, the test does not provide any fundamental property of asphalt binders.

Recently, the Federal Highway Administration (FHWA) proposed use of the repeated creep test to measure fundamental properties of asphalt binders; the test can also be used to identify the presence of modifiers (Bahia et. al., 2001). Therefore, the objective of this study was to evaluate the suitability of the repeated creep tests to identify the presence of modifier.

Typically, rutting is one of the major causes of premature failure of HMAC, especially within Texas. To identify rutting potential of HMAC, a Hamburg Wheel Tracking Device (HWTD) test has been specified by the Texas Department of Transportation (TxDOT). If HWTD test results identify a mix to be rut susceptible, the test results do not necessarily indicate whether the mix design or asphalt binder is the major factor responsible for rutting potential. It may be possible that the repeated creep test results can identify the rutting potential of the binder, thus identifying whether or not the asphalt binder is the contributing

factor. Therefore, another objective of this study was to identify the rutting potential of a mix consisting of rut prone asphalt binder using repeated creep tests. If a correlation can be established between the properties of the asphalt binders used in the HMAC and the rutting potential displayed in laboratory testing, premature failure can be minimized. It is expected that the addition of modifiers can significantly increase the binder stiffness at lower temperatures. To evaluate the increase in fatigue resistance and to make sure that the mixes are not brittle, the cracking potential of binder consisting of modifiers needs to be evaluated as well.

1.2 RESEARCH OBJECTIVE

The main objective of this research is to identify the presence of modifiers in the asphalt binders and determine their influence on the rut and fatigue potential of the HMAC specimen. By evaluating rheological properties of the binders and the rut depth potential of the HMAC specimens prepared with those binders, a relationship that can predict the rutting potential of HMAC placed in the future can be developed. The flexural beam fatigue beam test can be performed on the mixes to identify increase and decrease in cracking potential of HMAC. To perform this study, two mixes commonly used by TxDOT - Type-D and Coarse Matrix High Binder (CMHB-C) - were selected. The Type-D mix was obtained from the Austin District and the CMHB-C from the Bryan District. Both mixes have shown success in the field and have recently been placed using modifiers. The modifiers assessed in this study include Styrene-Butadiene-Styrene (SBS), Styrene-Butadiene-Rubber (SBR), Tire Rubber (TR), and Elvaloy.

To evaluate HMAC performance, the mixes were evaluated using the HWTD test (Tex-242-F), a test that has been very successful in Texas in the past. The HWTD tests were performed at the test temperature of 122 °F (50 °C) on 6 in. by 2.5 in. (150 mm by 62.5 mm) specimens. The mix is acceptable if rut depth is less than 0.5 in. (12.5 mm) after a specified number of wheel passes. The flexural beam fatigue tests were performed as per AASHTO T321-03 procedure and discussion on the procedure is included in Research Report No. 0-4824-2 (Rajpal et al., 2007).

To evaluate the presence of modifiers, the elastic recovery test (ASTM D 6084/ Tex-539-C) was performed at 50 °F (10 °C). To evaluate the permanent deformation potential of binders, the binders were evaluated in two different loading modes: frequency mode and repeated creep mode using Dynamic Shear Rheometer (DSR). DSR testing was performed at three temperatures: 126°F (52°C), 147°F (64°C), and 169°F (76°C) on specimens 1mm in height and 25mm in diameter.

1.3 ORGANIZATION

The introduction, research objectives and organization of the report are included in this chapter. Chapter Two discusses the background information on types of

modifiers and test procedures. Chapter Three discusses the mix design and tests performed in this research. Included in Chapter Four are the test results and analysis of the collected data, the results of validation efforts, and the elastic recovery test results. Conclusions and recommendations for future research are presented in Chapter Five.

CHAPTER 2 BACKGROUND

In this chapter, the background information is presented on the type of modifiers and their influence on the asphalt binder, along with the performance tests used for evaluation of asphalt binders and HMAC.

2.1 BINDER MODIFIERS

Modifiers are added to the asphalt to improve the performance of HMAC. Typically, modifiers are added to increase the stiffness at higher temperatures (Modifier B of Figure 2.1), thus increasing the resistance to permanent deformation (rut depth). It is possible that the increase in stiffness at high temperatures may increase stiffness at lower temperatures as well (Modifier A of Figure 2.1), which is less desirable because it can lead to thermal and/or fatigue cracking.

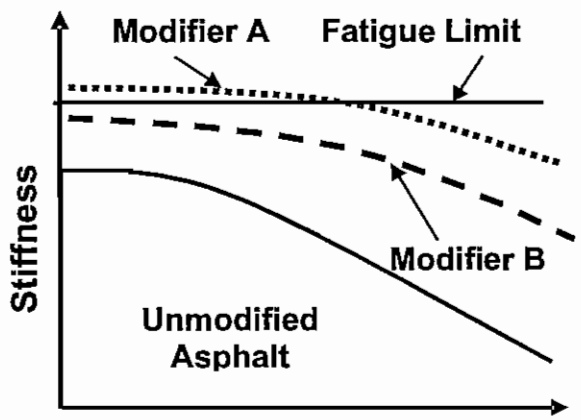

Figure 2.1 Influence of Modifiers on Binder

According to Maher (2000), modifiers can be classified into two groups: Type I Modified Binder and Type II Binder Modifier. Type I is a modifier that is premixed in the binder, while Type II is a modifier that is placed in the mix prior to placement in the field. Modifiers are added for various reasons in addition to increase in stiffness, as shown in Table 2.1.

The four main modifiers most commonly used by TxDOT - Styrene Butadiene Rubber (SBR), Styrene Butadiene Styrene (SBS), Elvaloy and Tire Rubber (TR) - mainly fall into the category of elastomers (Smit et al., 2004). Each of these modifiers increases the stiffness of the mix at higher temperatures, decreases the stiffness at lower temperatures and increases the elasticity in the medium range temperatures. All of the modifiers SBS, SBR, Elvaloy, and TR fall into the Type I

modifier category due to the fact that they are added when the binder is batched from the plant. These modifiers are beneficial for the purposes of this study because they improve binder performance at high service temperatures, and the rutting occurs at high temperatures.

Table 2.1 Types of Binder Modifiers (Roque, et. al., 2005)

Type	Purpose	Example
Filler	- Fill voids - Increase stability - Improve bond between aggregate and binder	- Lime - Portland Cement - Fly Ash
Extender	- Decreases the amount of asphalt cement needed (typically 20 - 35% of total asphalt binder)	- Sulfur - Lignin
Elastomers - Natural Latex - Synthetic Latex - Block, Di-Block Polymers - Reclaimed Tire Rubber	- Increase stiffness at higher temperatures - Increase elasticity at medium range temperatures to resist fatigue cracking - Decrease stiffness at lower temperatures to resist thermal cracking	- Natural rubber - Styrene-butadiene-styrene (SBS) - Crumb rubber (TR) - Styrene-butadiene rubber (SBR)
Fiber	- Improves tensile strength - Improve cohesion - Allow for higher asphalt content without draindown	- Asbestos - Polyester - Fiberglass
Plastomers (Thermoplastics)	- Increase high temperature performance - increase structural strength - increase resistance to rutting	- Ethyl-vinyl-acetate (EVA) - Polyvinyl chloride (PVC) - Ethylene propylene (EPDM) - Ethylene Acrylate Copolymer
Oxidant	- Increased stiffness after placement	- Manganese salts
Antioxidant	- Increase durability by retarding oxidation	- Leads - Carbons - Calcium salts
Hydrocarbons (Natural Asphalts)	- Restore aged asphalts - Increase stiffness	- Oils - Natural asphalts (Lake Asphalt) - Gilsonite
Anti-strippers	- Minimize binder stripping	- Lime - Amines
Waste Materials	- Replace aggregate with a cheaper product	- Roofing shingles - Recycled tires

2.1.1 *Styrene Butadiene Rubber (SBR)*

Styrene Butadiene Rubber (SBR) is a random polymer and the most commonly used type of synthetic rubber derived from the distillation process in oil refineries. SBR contains approximately 25% styrene and 75% butadiene, making a synthetic rubber with greater heat resistance but lower tensile strength than that of natural rubber. Figure 2.2 shows the basic chemical structure of the SBR polymer modifier.

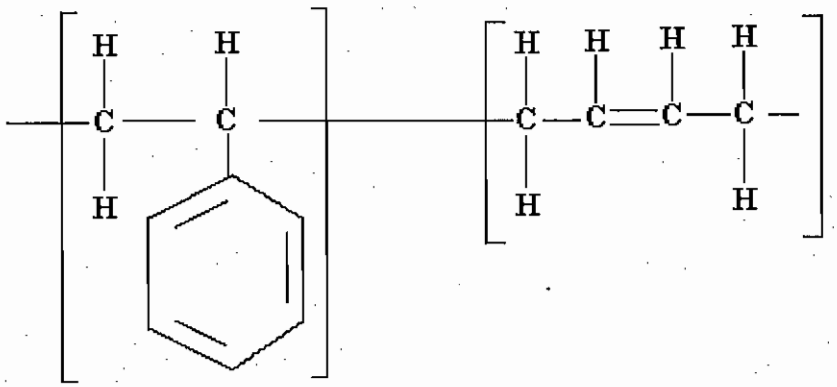

Figure 2.2 Chemical Structure of SBR Random Polymer (Rajpal, 2005)

2.1.2 *Styrene Butadiene Styrene (SBS)*

Styrene Butadiene Styrene (SBS) is a tri-block copolymer or a thermoplastic rubber. SBS significantly increases strength at higher temperatures as well as flexibility at lower temperatures. Figure 2.3 shows the basic chemical structure of the SBS polymer modifier.

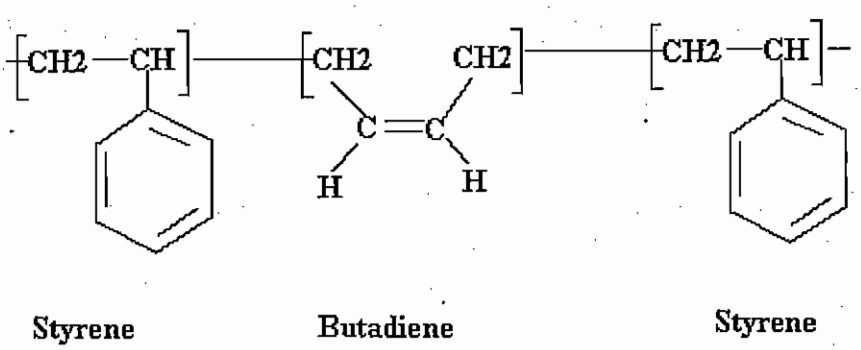

Figure 2.3 Chemical Structure of SBS Block Polymer (Rajpal, 2005)

2.1.3 *Tire Rubber (TR)*

Tire rubber, or crumb rubber, is a general type of asphalt modifier that contains scrap tire rubber. Tire Rubber (TR) or Ground Tire Rubber (GTR) is a polymer that is often referred to as a thermoset and is used for various types of mixes. Thermosets are differentiated from elastomers in that they are more rigid, tightly crossed linked polymers that degrade rather then melt upon the application of heat (Kraier et al, 1988).

2.1.4 *Elvaloy*

The information about the Elvaloy was obtained from the DuPont website (www.dupont.com/industrial-polymers/elvaloy.) and is reproduced in the following paragraph, with its chemical reaction mechanism displayed in Figure 2.4.

Elvaloy is a random terpolymer comprising ethylene, normal butylacrylate and glycidyl methacrylate (GMA). The molecular weight and co monomer levels can be varied during polymer manufacture. Added in small quantities to asphalt, Elvaloy terpolymer creates a permanently modified binder with improved elastomeric properties. Unlike most other plastomers and elastomers that are simply mixed into asphalt, Elvaloy has an active ingredient that chemically reacts with asphalt. The result is not a mixture of asphalt and modifier, but rather a stable, elastically improved, more resilient binder that can be stored and shipped to hot mix plants to help meet SHRP and other higher-performance specifications. It is the GMA portion of the molecule that appears to be responsible for the reaction observed when Elvaloy is mixed and heated with asphalt. Elvaloy copolymers chemically react with asphalt to form a polymer-linked-asphalt system with improved performance properties; Figure 2.4 represents the reaction mechanism of elvaloy with asphaltene.

The epoxide ring in the glycidal structure is believed to undergo an addition reaction with various functional groups in a typical asphaltene molecule. The asphaltenes, which can have carboxylic acid functionality, open the epoxy ring and form an aromatic ester. Polymers with higher levels of GMA have been and evaluated in asphalt. These polymers appear to allow the use of fewer polymers to give the same response in high temperature SHRP properties. Hot mix asphalts made with Elvaloy are easy to spread and compact, and provide outstanding resistant to rutting, cold cracking and fatigue. Roads made with Elvaloy have been in service since 1991, and are showing excellent long-term durability.

To evaluate the capabilities of the modifiers, several test procedures have been developed. To identify rutting and cracking potential of HMAC mixes, the identified test procedures for asphalt binder and HMAC specimens should be able to predict the resistance to permanent deformation and cracking. The identified test procedures are included in the following sections.

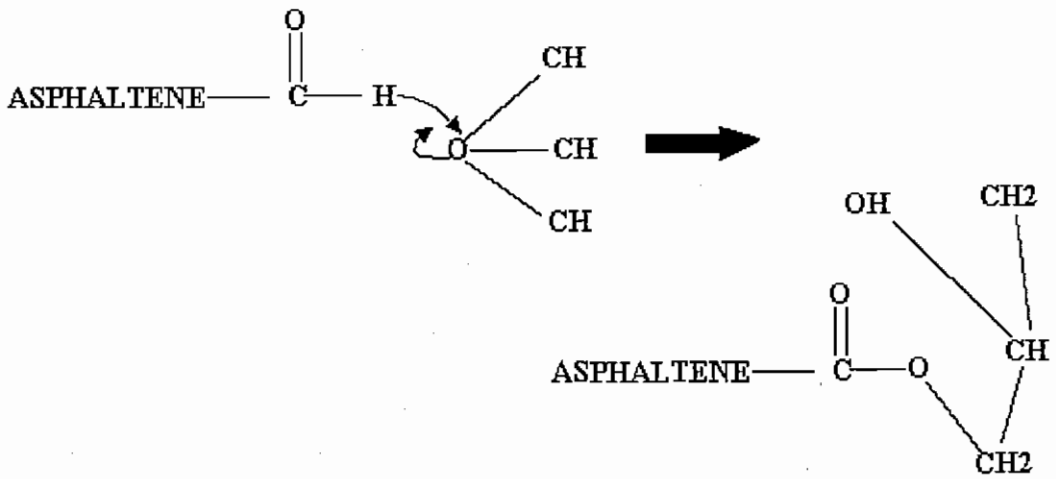

Figure 2.4 Reaction Mechanism of Elvaloy with Asphaltene

2.2 HMAC PERFORMANCE TESTS

Although various test methods are currently available to identify rutting potential of HMAC, the HWTD was selected in this study due to the fact that TxDOT specifies this test procedure to evaluate rutting potential of HMAC. In terms of fatigue cracking, the flexural beam fatigue test specified by AASHTO (AASHTO T321-03) was used in this study and details of the test procedure are included in Rajpal et al. (2007).

2.2.1 Hamburg Wheel Tracking Device (HWTD) – (Tex-242-F)

The HWTD, illustrated in Figure 2.5, measures the combined effects of rutting and moisture susceptibility of an asphalt concrete mix. Steel wheels roll across the HMAC surface that is typically submerged in water and the susceptibility to rutting is identified based on a pass/fail criterion specified by TxDOT.

The HWTD was desigued in the 1970's by Esso A.G. of Hamburg, Germany, and was based on a similar British device that incorporated a rubber tire (Aschenbrener, 1995). Initially, the number of passes was set to somewhere around 10,000 at a temperature of 40 to 50°C. When it was noted that some specimens experienced major moisture damage shortly after the 10,000 cycle mark, the number of cycles was raised to 20,000. TxDOT evaluates different PG mixtures at different number of cycles (Table 2.2) with the maximum deformation being 12.5mm for all binder types.

Figure 2.5 Hamburg Wheel Tracking Device and Computer Setup

Table 2.2 TxDOT Specifications for Hamburg Wheel Tracking Device

High Temperature PG Grade	Number of Passes[1] for Max. Deformation of 12.5 mm
64	10,000
70	15,000
76	20,000

[1] May be decreased or waived when shown on plans

The only disadvantage of this test is that it does not provide a fundamental property that can be used for modeling purposes. Recommended values for specific climates and traffic levels are also not available. However, the test is easy to perform and is part of TxDOT acceptance criterion (ITEM 341, 344, and 346).

2.3 PERFORMANCE TESTS FOR ASPHALT BINDER

To move towards performance based specifications and measure rheological properties, a Dynamic Shear Rheoemeter (DSR) has been adopted by state highway agencies throughout the country. The DSR (Figure 2.6) measures rheological properties of asphalt binder rather than empirical properties such as penetration values or softening point. Measurements can be performed at various temperatures, strain and stress levels, and frequencies. In the SHRP asphalt binder specifications, the DSR is used to predict the fatigue and rutting potential of the binder (Youtcheff, 1994).

Figure 2.6 Dynamic Shear Rheometer

Although SHRP specifications suggested performing a test at fixed frequency, the system can be upgraded to perform a series of tests. The most commonly used tests are oscillation or frequency, zero shear viscosity, and repeated creep (Bahia et al. 2001; Marasteanu, et al., 2005). Oscillation tests can be performed at various temperatures and stress or strain levels. In the oscillation mode, the DSR can also be used to determine the frequency dependency of the modulus of asphalt binders by performing a frequency sweep. In viscosity mode, the tests are performed as a function of shear rate, shear stress, temperature and time. Finally, the repeated creep tests are performed to identify compliance of the asphalt binder and accumulation of permanent strain due to load repetition.

In recent research efforts, it has been identified that the rutting parameters that are currently being used, $G^*/\sin\delta$, for PG specifications do not accurately predict the rutting potential of HMAC, especially when modifiers are used (Marasteanu, et al., 2005). Other parameters being investigated include zero shear viscosity and permanent strain under repeated creep and recovery testing (Marasteanu, et al., 2005).

In Europe, zero shear viscosity is being proposed as a high-temperature specification parameter. Zero shear viscosity (ZSV), used as a specification criterion for asphalt binders, was implemented when the inability of the Superpave criterion $G^*/\sin\delta$ was identified (Anderson et. al., 2002). ZSV has the ability to capture the contribution to rutting resistance afforded by polymer modification. ZSV can be determined directly from long-term creep tests, but such tests are time-consuming and are often very difficult to perform (Anderson et. al., 2002).

In this study, the DSR is used to perform frequency sweep and repeated creep tests. The ZSV test was not performed due to project constraints. The frequency sweep tests were performed to identify complex shear modulus and phase angles of asphalt binders. The repeated creep tests were performed at various stress levels before selecting a fixed level to determine the resistance of an asphalt

binder to permanent deformation under repeated loading that is meant to simulate traffic loading. A brief discussion about each test is provided in the following section.

2.3.1 Frequency Sweep

Although the PG specifications suggest performing tests at one frequency, the test can be repeated for a range of frequency and is termed as a frequency sweep test. The frequency sweep test yields a number of parameters related to the binder being tested: complex modulus, viscous modulus, elastic modulus, and phase angle. The two parameters of most concern are the complex modulus (G*) and the phase angle (δ). With these two parameters G*/sinδ value can be estimated. G*/sinδ is an indicator of rutting potential of tested binder (Seeds, 1998). G* is a measure of the total resistance of a binder to deformation when exposed to repeated pulses of shear stress. It consists of both a storage modulus (G') and non-recoverable loss modulus (G"), as shown in Figure 2.7.

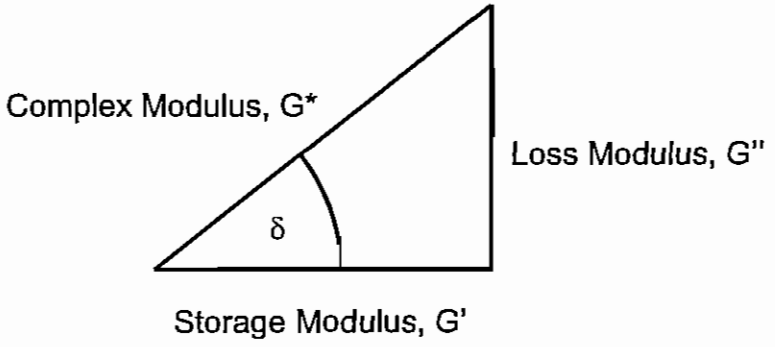

Figure 2.7 Components of Complex Shear Modulus

On the other hand, δ is the arc tangent of the ratio of loss over storage modulus indicating level of viscous component present in the binder. Thus, ratio of G*/sinδ is an indicator of the amount of non-recoverable deformation. A typical example of applied shear load and measured response is shown in Figure 2.8. The solid line represents applied stress and the dashed line represents measured strain. The time lag in measured strain with respect to applied stress is an indicator of the presence of viscous components (δ).

The G* measured at various frequencies can be represented in terms of horizontal (storage modulus, G') and vertical components (loss modulus, G") using the relationship presented in Figure 2.7. A typical relationship between the two components is shown in Figure 2.9. High values of G* and low values of δ are desirable from the standpoint of rut resistance and are used in the determination of the performance grades (PG) of binders.

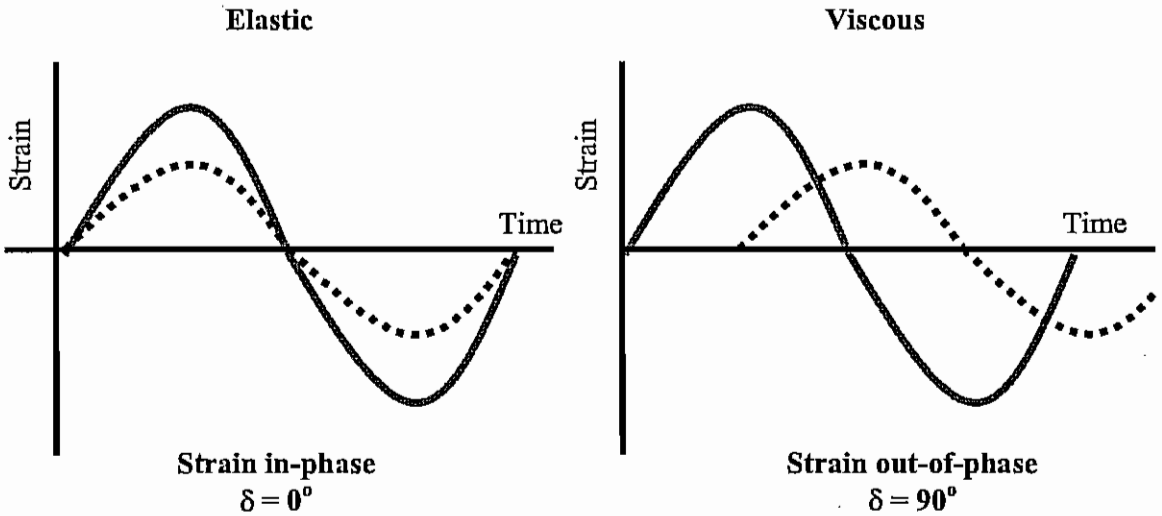

Figure 2.8 Determination of Phase Angle, δ

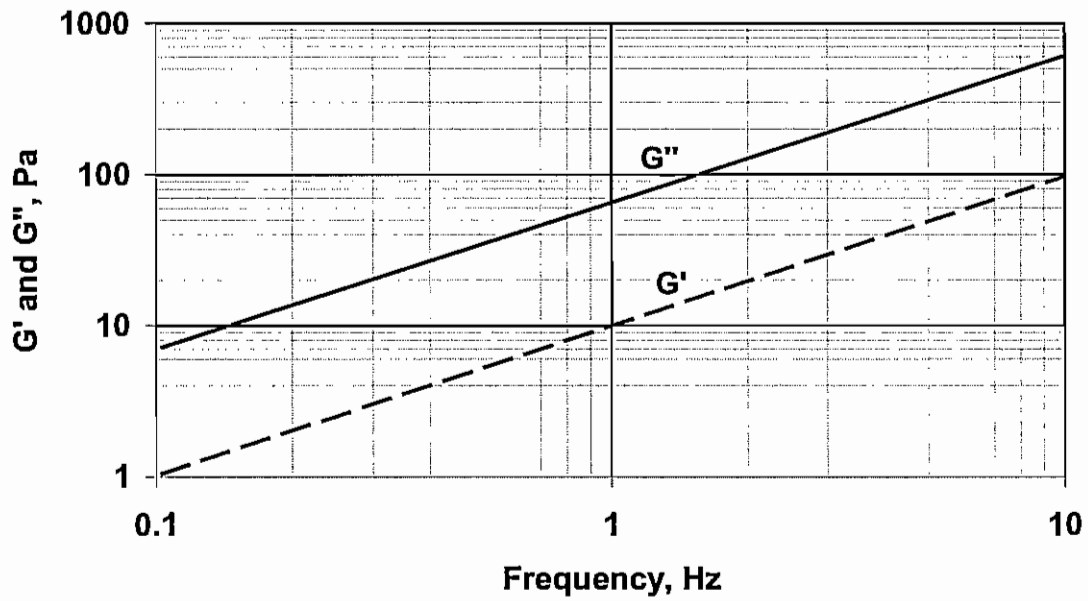

Figure 2.9 Vertical and Horizontal Components of Complex Modulus,

2.3.2 Repeated Creep

Creep tests give important and practical information in regards to the mechanical properties of asphalt binders (Herh, 1997). It is expected that flexible pavements should return to their original state after removal of applied load to avoid permanent deformation. However, in reality the pavements do not regain their original shape due to the presence of viscous components in asphalt binder. The component of interest in this research is the presence of asphalt binder which is a

viscoelastic material. Rutting (permanent deformation) in the top layer of flexible pavements (i.e., HMAC) can be attributed to the accumulation of permanent strain due to repeated application and removal of traffic loads. The repeated creep test can simulate the field conditions (Bahia et al., 2001). The ability of the binder to recover after removal of load depends on the magnitude of loss modulus which can be modified in the presence of additives.

The repeated creep test is typically performed by applying load for 1 second and waiting for 9 seconds before application of load again. Therefore, a loading cycle is completed in 10 seconds (Figure 2.10). The data presented in Figure 2.10 shows the load application for 3 cycles. The test procedure suggests that the tests be performed for 100 cycles (Bahia et al., 2001). The unrecoverable deformation at the end of each cycle is accumulated to identify permanent deformation at the end of fifty cycles. The loads can be varied to a range of magnitudes to identify the influence of load levels on the accumulated strain.

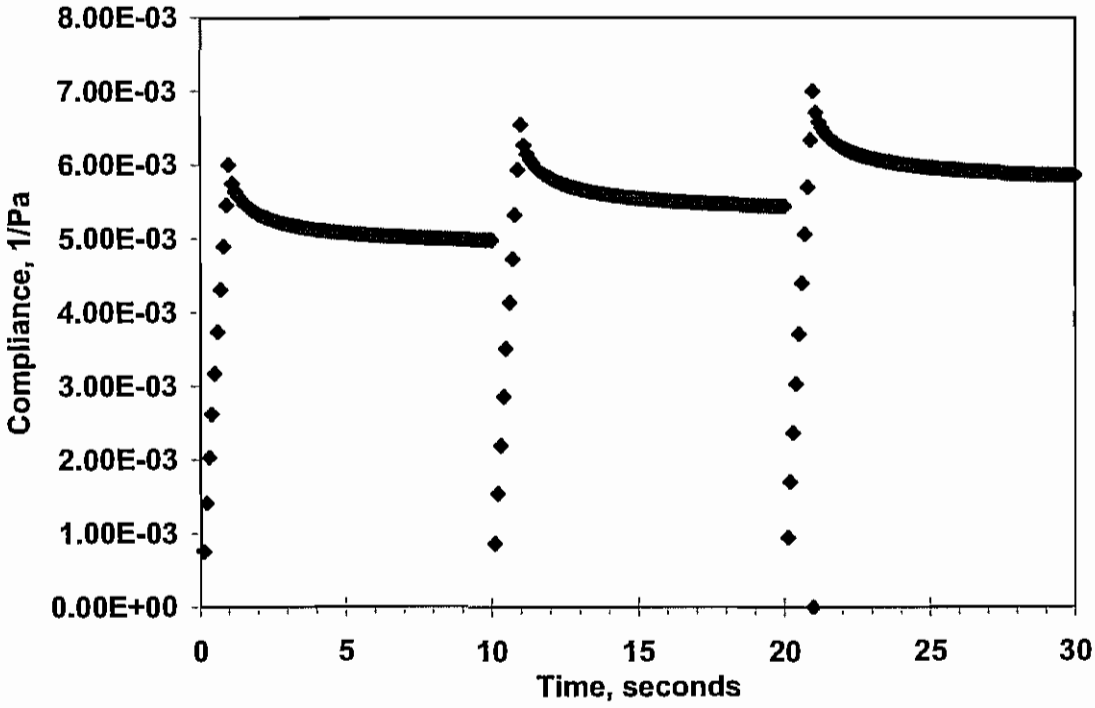

Figure 2.10 Loading and Unloading of Asphalt Binder for the First Three Cycles

Binders subjected to repeated creep testing most accurately simulate the loading of pavements due to traffic and therefore can provide useful information and make up for the short comings that are found while using $G^*/\sin\delta$ as a rut indicator. Bahia et al. found that the $G^*/\sin\delta$ parameter did not show reasonable correlation with the mixture rutting performance for two main reasons. First, $G^*/\sin\delta$ is derived from the linear viscoelastic response measured after only a few cycles of testing, which does not allow for the full measurement of the damage

behavior of the binders. Second, G*/sinδ is derived from cyclic reversible loading that does not allow for a direct measurement and is not a good scientific indicator of the accumulation of permanent strain during creep loading. The utilization of a repeated creep test solved both problems. Repeated creep can measure the damage behavior in both the linear and nonlinear range (Bahia et. al., 2001).

2.3.3 Elastic Recovery Test

The elastic recovery test describes the method of measuring the recovery of tensile deformation of an asphalt sample by using a standard ductilometer. Currently, TxDOT uses a modified version of ASTM D 6084 procedure for performance grade (PG) binders and uses Tex-539-C for evaluating AC grade binders. The methods use a ductilometer to stretch a sample at a constant deformation rate of 50 mm per minute. The elongation used in ASTM D 6084 method is 100 mm (4 in), whereas the elongation for Tex-539-C is 200 mm (8 in). At this elongation the specimen is cut and allowed to relax for 60 minutes. During this relaxation period, the sample tends to recover elastically in that the ends of the cut sample will draw apart. The distance between the ends of the cut sample after the 60 minute relaxation period is the elongation after elastic recovery. Elastic recovery is calculated as the ratio of the difference between the original elongation (100 mm or 200 mm) and the elongation after elastic recovery. The tests are performed at 10 °C (50 °F). This test is currently part of TxDOT specifications and, being one of the objectives of this study, was used for identifying the presence of modifier.

2.3.4 Fatigue Evaluation

To evaluate fatigue resistance of binder, it was decided to use G*xsinδ value as specified by SHRP. The specifications suggest that the complex modulus tests be performed on the long term oven aged binders at the temperature depending on the PG grade. A value of G*sinδ greater than 5,000 kPa indicates that the material is prone to cracking. Although Bahia et al. (2001) have proposed news tests to evaluate fatigue cracking potential of binders, the tests were not performed due to project constraints.

2.3.5 Other Binder Specification Criterion

Various parameters have been proposed to improve the current Superpave high-temperature binder specification (Dongre, 2003). One parameter relates the phase angle (δ) directly to accumulated strain from the creep-recovery test. Another variation suggests a formula to predict the accumulated strain using the current Superpave parameters G* and sinδ. Recently, NCHRP Project 9-10 suggested a criterion based on a parameter derived from Burger's viscoelastic model (Dongre, 2003). However, these parameters were not evaluated in this study due to time constraints.

Based on the discussion, an experiment design was formulated to achieve the objectives of the study and is presented in the following chapter.

CHAPTER 3 MATERIAL PROPERTIES AND TEST SETUPS

3.1 MATERIAL PROPERTIES

To evaluate the influence of binder on permanent deformation, two mix types and ten binders were selected and tested. The mix design, asphalt binder properties, and test procedures used for the evaluation are presented in this chapter.

3.1.1 Mix Design and Binder Types

Two commonly used surface mixes: Type-D and Coarse Matrix High Binder (CMHB-C) were selected for this study. The Type-D mix was obtained from the Austin District, while CMHB-C mix was obtained from the Bryan District. Historically, both mix types have performed well. To make sure that the mix design evaluated in the laboratory is similar to the placed mixes, the Job Mix Formula (JMF) of recently placed mixes was acquired from TxDOT and is summarized in Table 3.1. The binder content of CMHB-C is slightly higher than Type D mix (Table 3.1), while the aggregate gradation of two mixes is significantly different as shown in Figures 3.1 and 3.2, respectively. CMHB-C is a gap graded mix design containing a large quantity of coarse aggregate with asphalt binder-filler mastic. CMHB-C mixtures have been known to be more resistant to moisture and rutting in the field. Type D mix consists of a maximum aggregate size of ½-inch and is most commonly used in the overlay layer placement (TxAPA, 2005).

The properties of four modifier types used in this study are summarized in Table 3.2. To ensure that the influence of modifier was evaluated, original (unmodified) binder was obtained from the manufacturers. In addition, an attempt was made to obtain binder (both modified and unmodified) that had been or would be placed on the highways to ensure that incompatible asphalt binders were not obtained. The only exception to this rule was the asphalt binder obtained from BASF, where the asphalt producer was asked to mix a SBR modifier.

The asphalt binders obtained from Wright and Ultrapave provided Superpave gradation and are included in the Table 3.2. The asphalt binders obtained from Valero Armor and BASF did not provide the gradation; therefore, the limited available test results are included in the table. The results indicate that the asphalt binder meets the PG specifications.

Table 3.1 Job Mix Formula for Type D and CMHB-C Mix Designs

Binder Grade	PG 64-22, PG67-22, PG70-22, PG76-22	
Mix Type	Type D	CMHB-C
Binder Content,%	4.5	4.9
Sieve Size	Percent Passing	
3/4	100.0	100.0
1/2	100.0	100.0
3/8	97.0	61.0
No. 4	65.0	34.8
No. 10	35.5	20.4
No. 40	17.1	11.6
No. 80	6.6	8.8
No. 200	2.6	7.0
Maximum Specific Gravity	2.550	2.423
Aggregate Bulk Specific Gravity	2.655	2.591
Air Voids	4.0	4.0
VMA	14.3	17.6
VFA	71.9	77.3
V_{eff} %	3.6	3.7

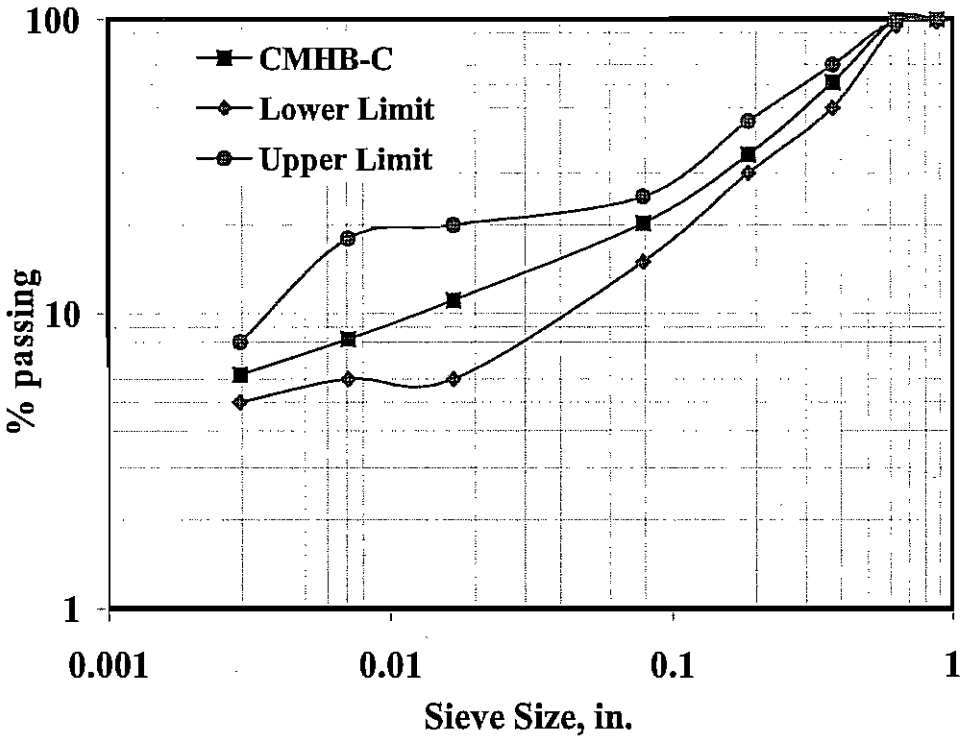

Figure 3.1 CMHB-C Gradation

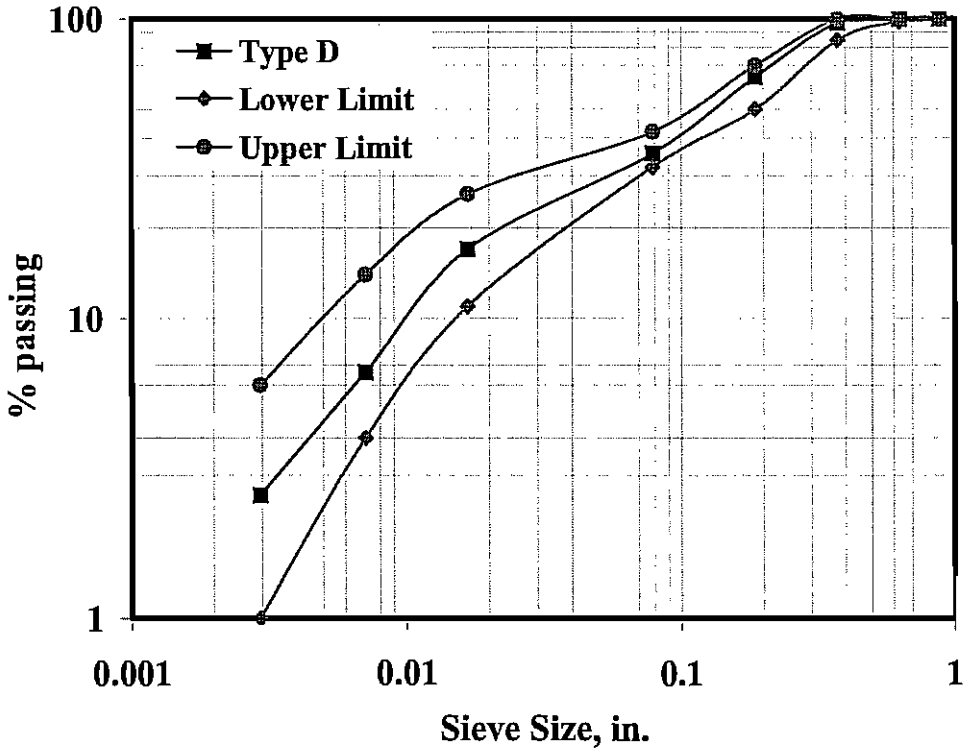

Figure 3.2 Type D Gradation

Table 3.2 Rheological Properties of Asphalt Binders

Asphalt Producer	Wright Asphalt			Ultrapave		Valero Armor			BASF	
PG grade	64-22	70-22	76-22	67-22	76-22	64-22	70-22	76-22	64-22	70-22
Modifier	0%	3.0% SBS	SBS+TR	0%	3.5% SBR	0%	2.0% Elvaloy	3.5% Elvaloy	0%	2.0% SBR
Rotational Viscosity, @ 135°C	0.53	1.4	2.133	0.587	1.367	1.025	0.855	5.122	1.110	0.742
Softening Point, F	0.23	137	153	N/T	N/T*	N/T	N/T	N/T	N/T	N/T
Penetration @25 °C	61	56	52	N/T	N/T	N/T	N/T	N/T	N/T	N/T
G*/sinδ @ 10rad/sec, kPa	1.75	1.517	1.329	2.5	3.02	1.78	1.5	2.34	0.54	0.75
Phase Angle @ 10 rad/sec.	84.6	74.2	69.1	81.1	70.7	81.7	78.2	72.2	75.1	74.7
Specific Gravity @ 60°F	1.04	1.038	1.039	N/T	N/T	N/T	N/T	N/T	N/T	N/T
Elastic Recovery @ 10°C	N/A	52.5	62.5	N/T	N/T	N/T	54.7	54.7		
RTFO Aging	N/T									
G*/sinδ 10rad/sec, kPa	4.47	3.388	2.958	6.35	10.6	4.16	3.59	6.53	0.68	0.81
Phase Angle @ 10 rad/sec.	79.8	69.8	66.8	85.2	85.4	85.3	73.2	67.2	73.0	72.1
Change in mass	0.02	0.019	0.02	N/T	N/T	N/T	N/T	N/T	N/T	N/T
PAV Aging	N/T									
G*/sinδ @ 10rad/sec, kPa	1978.9	2184.8	2374.8	3086	2585	N/T	N/T	N/T	N/T	N/T
S, -12 °C @ 60sec	147.2	1.335	107.4	122	114	N/T	N/T	N/T	N/T	N/T
m, -12 °C @ 60sec	0.3137	0.3283	0.3135	0.325	0.317	N/T	N/T	N/T	N/T	N/T

* Not Tested

Although different binders were evaluated in this study, the binder contents of Type-D and CMHB-C mixes were not changed from the original JMF. It is quite possible that the change in binder types can alter the optimum binder content; however, the change in binder content can influence rutting or cracking potential of mix types. Therefore, it was decided to maintain the binder content constant. Another thing to keep in mind is that the modifiers typically improved the higher temperature grade while maintaining the lower temperature grade of -22, indicating that the modifiers mainly improved performance at higher temperature.

3.2 SPECIMEN PREPARATION AND TEST PROCEDURE FOR HWTD

3.2.1 Specimen Preparation

All HWTD specimen preparation was performed in accordance with TxDOT's Tex-242-F. Mixing and compaction temperatures were identified by performing viscosity tests specified by SHRP using Brookfield Viscometer. The estimated mixing and compaction temperatures for individual binder types are summarized in Table 3.3.

Table 3.3 Mixing and Compaction Temperatures for Individual Binder Types

Binder	Mixing Temperature (°F)	Compaction Temperature (°F)
Wright Asphalt 64-22	300-310	275-285
Wright Asphalt 70-22 3.5% SBS	330-340	300-310
Wright Asphalt 76-22 SBS & TR	330-340	300-310
Valero Armor 64-22	300-310	275-285
Valero Armor 70-22 2% Elvaloy	330-340	300-310
Valero Armor 76-22 3.5% Elvaloy	325-335	300-310
Ultrapave 67-22	310-320	290-300
Ultrapave 76-22 3.5% SBR	325-335	300-310
BASF 64-22	300-310	275-285
BASF 70-22 2% SBR	330-340	300-310

Mixing is done in a large mechanical mixer to thoroughly mix the asphalt binder and aggregates. After mixing is complete, the loose mix is placed in an oven to induce short term aging. Short term oven aging simulates the induced aging during production and placement of HMAC. The short term aging period specified by TxDOT is 4 hours for the Type D mix and 2 hours for the CMHB-C mix.

During the short term aging period, the specimens are stirred every 30 to 60 minutes to ensure uniform aging throughout the mix. Compaction is then performed using the Superpave Gyratory Compactor (SGC). The mold and the plates are heated in the oven at the specified compaction temperature to ensure

that the mix temperature is not reduced. The amount of loose mix required for specimen preparation is calculated based on maximum theoretical specific gravity (G_{mm}) of the loose mix. The estimated weight is placed into the mold, which is placed inside the SGC, and the specimen is then compacted to the desired height.

To perform HWTD tests, four specimens are compacted to a density of 93 ±1% using a SGC. The compacted specimens, which are 6 in. (150 ±2 mm) in diameter by 2.5 in. (62 ±2 mm) in height, are cooled to room temperature for a period of 24 hours. The four specimens are then divided into two groups. The edge of each specimen is then trimmed with a masonry saw. The trimming is approximately $^5/_8$ in. (16 mm), as shown in Figure 3.3, so that the two specimens are flush with each other to form one uniform specimen. The specimens are placed in an acrylic mold and then placed in a mounting tray. The thickness of the acrylic mold is 2.4 in. (60 mm). The specimens in the mold are labeled with the percent air voids, mix type and height.

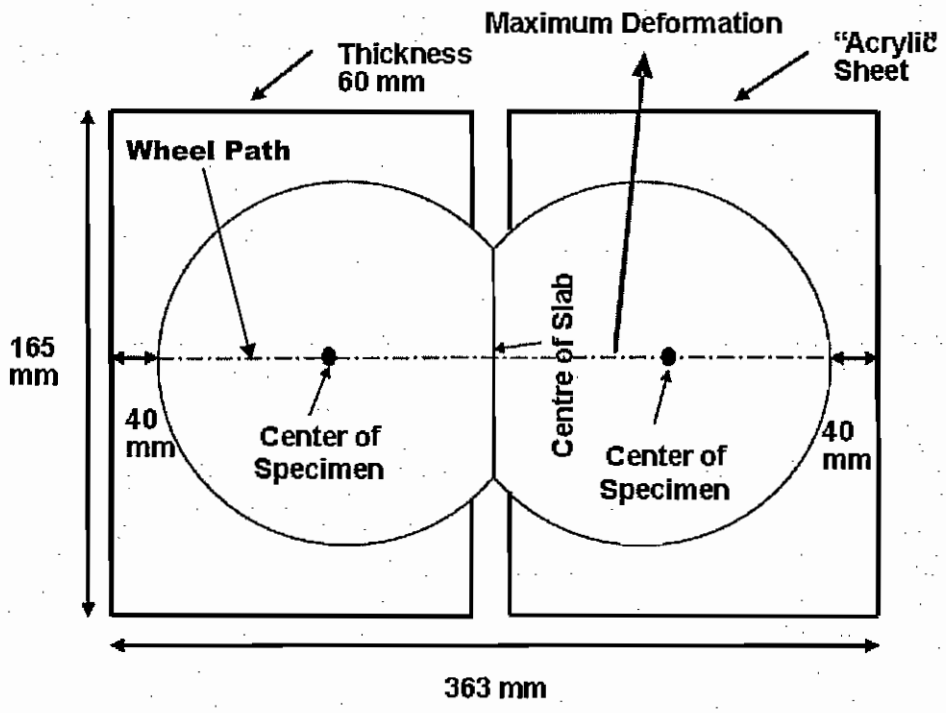

Figure 3.3 HWTD Specimen Setup

The HWTD tests two uniform specimens simultaneously with two reciprocating solid steel wheels. Initially the test was designed for slab specimen testing but was converted to cylindrical specimen testing with the invention and increasing use of the SGC (Izzo and Tahmorrasi, 1999).

The wheels have a diameter of 8 inches (204 mm) and a width of 1.85 inches (47 mm). The load is fixed at 685 N, and the average contact stress given by the manufacturer is 204 MPa (Romero, 1998). Given that the contact area increases

with rut depth, contact stress is variable. According to the manufacturer, a contact stress of 0.7 MPa approximates the stress produced by one rear tire of a double-axle truck. The average speed of each wheel is approximately 1.1 kilometers per hour which is equivalent to 53 ± 2 wheel passes per minute (Aschenbrener, 1995).

Information regarding the specimens and water temperature is entered into the computer. The mounting trays are then fastened to the empty water bath. The water bath is filled with water and heated to 122°F (50°C). The test specimens are allowed to saturate in the water bath for an additional 60 minutes once the 122°F (50°C) water temperature is reached. This waiting time is also referred to as start delay time. Once the test starts, the specimens are maintained in the water for 307 minutes. The test is automatically stopped when the required number of passes or the maximum allowable rutting depth of 0.5 in. (12.5 mm) is reached. For each specimen, the number of passes to failure or the final rut depth is recorded.

According to TxDOT specifications, the maximum rut depth anywhere in the wheel path should be measured (Tex 242-F). The two merged specimens are broken down into two sections. The average value measured at the center of each specimen is calculated and reported as the center of the specimen deformation. The deformation is measured at the center point between the two merged specimens and reported as the center of slab deformation. A study was conducted by Joe Button at the Texas Transportation Institute (TTI) in which it was identified that measuring the rut depth at the center of the specimen provides a more repeatable rut depth measurement. Maximum rut can occur at any point on the combined specimen but is usually seen in the central area of the two specimens because there is less confinement in this area as opposed to the rest of the specimen, also resulting in a higher concentration of data points recorded in the central area of the two specimens. For our study the rut depths were compared at three locations across the specimen: the middle of each specimen and the center of the slab, from Figure 3.3. Both the average of the middle of the specimens and the center of the slab measurements were compared against the overall maximum deformation observed throughout the entire specimen, which can occur at any point.

As previously discussed, the number of cycles is dependent on the type of binder used in the mix. All tests were performed until 20,000 cycles regardless of the binder type to provide uniformity for future analysis purposes.

3.3 SPECIMEN PREPARATION AND TEST PROCEDURE FOR FLEXURAL BEAM FATIGUE TESTS

The specimen preparation and test procedure for flexural beam fatigue test process is included in Research Report No. 0-4824-2 (Rajpal et al., 2007).

3.4 ROLLING THIN FILM OVEN AGING PROCEDURE FOR ASPHALT BINDERS

Since the binder used in preparing the HWTD specimens has been short term aged in the specimen preparation process, the binder tested in the DSR needs to be aged as well to simulate the short term aging. The Rolling Thin Film Oven (RTFO) aging procedure is a conditioning step that models the construction aging of asphalt binder. That is it simulates the time that lapses between the batching of the binder, transportation and placement.

The RTFO consists of an oven chamber with a vertical circular carriage that rotates while housing the sample bottles containing the asphalt binder (see Figure 3.4). A fan circulates air in the chamber that is maintained at 325 °F (163 °C) and a jet blows air into the sample bottles as they rotate around the chamber.

A minimum of 12.4 oz. (350 grams) of asphalt binder is heated until fluid to pour inside a sample bottle. One sample bottle is placed on the scale and the scale is zeroed before pouring 1.24 oz. (35 grams) of binder into the bottle. The sample is then cooled to room temperature in the glass sample bottle. This is repeated until all 8 sample bottles are filled and cooled. The bottles are then placed in the sample rack in the oven and the oven door is closed. The rotation and air flow are then begun at 15 ±0.2 rpm and 4000 ±200 ml/min (0.004 ± 0.0002 m^3) respectively. The samples are then aged in the oven for 85 minutes with the air flowing, the carriage rotating and the proper temperature regained within the first 10 minutes of testing. The bottles are then removed and two are set aside for mass change determination. The remaining bottles containing the aged binder are then emptied into a suitable container and set aside for further DSR testing.

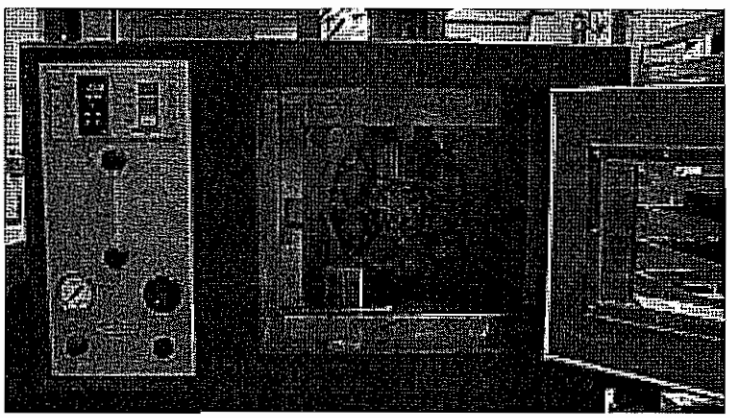

Figure 3.4 Rolling Thin Film Oven

3.5 DSR TEST PROCEDURE AND SPECIMEN PREPARATION

In this study, the DSR tests were performed using parallel plate arrangement. The diameter of the plate was 25 mm and the gap between top and bottom plate was set at 1 mm. The test specimens were prepared as per the AASHTO TP-5 procedure. Temperature is the most important factor when performing a DSR test. As it has been documented, asphalt binders are susceptible to temperature and the variance of just 1°C in DSR testing can lead to significant variations in the viscosity of the binder being measured (Carswell, 1995). The second most important thing is the gap between the top and bottom plate. It is essential that the gap is set to the specified width of 1 mm because an incorrect gap will affect the measurements.

3.5.1 Repeated Creep Test

In this study, the repeated tests were performed at three temperatures: 126°F (52°C), 147°F (64°C), and 169°F (76°C) regardless of modifier type. The repeated creep tests were performed at a constant stress for 1-s followed by a rest period of 9-s (zero stress), which is considered to be one cycle. During the 9-s rest period, the specimen recovers some of the strain that was developed during the 1-s stress period before it is loaded again (Button, 2004). A total of 100 creep and recovery cycles were performed on the unaged and RTFO aged binders. The applied shear stress was varied from 25 to 3,200 Pa. Each specimen was tested three times and the average value plotted in order to ensure that the measurement was correct and repeatable.

3.5.2 Frequency Sweep Test

The frequency sweep tests were performed for frequencies ranging from 0.01 to 24.1 Hertz and measurements were taken at 20 different intervals between the two frequencies. The test temperatures were similar to that of repeated creep tests.

3.6 ELASTIC RECOVERY TEST PROCEDURE AND SPECIMEN PREPARATION

The elastic recovery test describes the method of measuring the recovery of tensile deformation of an asphalt sample. The ductilometer is used to stretch a sample at a constant deformation rate of 50 mm per minute (2 in./min). Since ITEM 300 specifies usage of ASTM D 6084 for PG grade binders and all of the asphalt types used in this study were PG grade, the specimen is elongated to only 100 mm (4 in). At the end of elongation, the specimen is cut and allowed to relax for 60 minutes. During this relaxation period, the sample is expected to recover elastically. The two halves are moved together until the cut ends of the sample meet. The distance between the ends of the cut sample is the elongation after elastic recovery. Elastic recovery is calculated as the ratio of the difference between the original elongation (100 mm) and the elongation after elastic recovery. The procedure suggests performing tests at 10 °C (50 °F) and holding

the elongated specimen for 5 minutes before cutting. If the elastic recovery is less than specified minimum (depending on PG grade), then the asphalt binder fails the specifications.

The specimens for this test are prepared as per AASHTO T 51 and the mold used for testing specimen is shown in Figure 3.5. In this study, samples were tested at 50 °F (10 °C). To calculate percent elastic recovery, the following equation was used:

$$R = \frac{(100 - E_f)}{100} * 100 \qquad \text{(Equation 3.1)}$$

Where
R = the elastic recovery
Ef = the final elongation at the end of the test in mm.

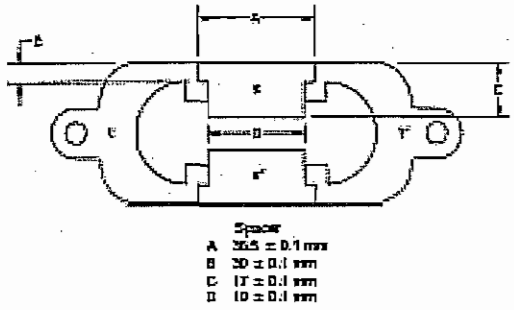

Figure 3.5 Mold for Elastic Recovery Tests

CHAPTER 4 DATA ANALYSIS AND TEST RESULTS

4.1 HAMBURG TEST RESULTS

The HWTD testing was conducted in accordance with TxDOT Tex-242-F specifications. The deformation of HMAC with number of cycles was recorded at the center of specimen and center of slab as suggested in Figure 3.3 as well as the maximum rut depth anywhere in the wheel path. The deformation of HMAC with number of cycles recorded at the two locations is reported in Figures 4.1 and 4.2. The results indicate that deformation is of similar magnitude at both locations. However, the deformation measured from the two wheels is slightly different when the data from center of slab is recorded (Figure 4.1), while it is identical when measured at the center of specimen (Figure 4.2). The trend is similar to those observed by Rajpal (2005).

To improve clarity of the data, it was decided to curve fit the data using polynomial fit. Initially, a 6th degree polynomial fit was plotted with the given data but was eventually reduced to 3rd degree, which gave a reasonable trend of the observed deformations in the specimens. The R^2 value throughout all the test data was never found to be less than 0.97 indicating that the 3rd degree polynomial fit is reliable. Also shown in the figures is the limitation of the polynomial fit of the data. Initially in the first few hundred cycles, the curve does not fit the data well; however, this is not a concern because the main focus of the testing is the ultimate rut depth at 20,000 cycles rather than initial rut depth. For clarity and ease of analysis, the HWTD plots will only include the 3rd degree polynomial fit and exclude the original data as it clutters the figure when more than one set of data is plotted. To minimize clutter due to labeling, it was decided to abbreviate the binder types, and the acronyms are included in Table 4.1

The HWTD test results for the Type D and CMHB-C mix designs at the center of the slab are reported in Figures 4.3 and 4.4; the deformations observed at the center of specimens are reported in Figures 4.5 and 4.6. In addition, the maximum deformation observed anywhere on the wheel path (Figure 3.3) are reported in Figures 4.7 and 4.8. Since TxDOT specifications are based on maximum deformation, this data is also included in the analysis. The estimated rut depth at the end of 20,000 cycles or when the device stopped after excessive deformation is summarized in Table 4.2.

The binders including modifiers demonstrated a smaller deformation than the base binders from the same producer throughout all of the testing. Thus, it can be stated that the modifiers improved the rut resistance of the specimens in all cases in which they were used.

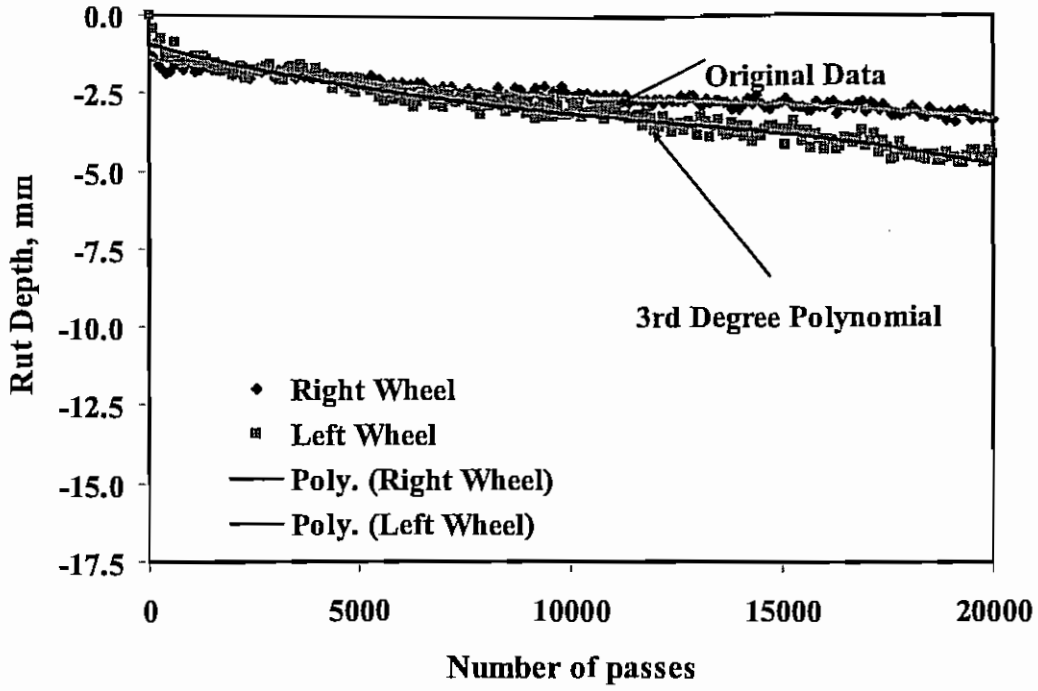

Figure 4.1 Typical Hamburg Wheel Tracking Device Test Results for Center of Slab

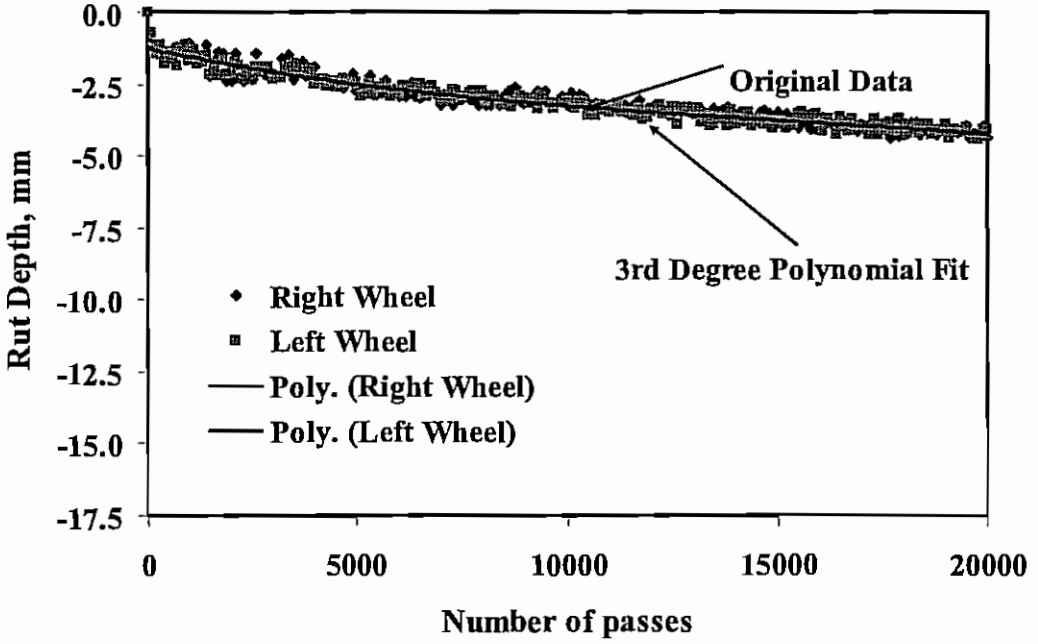

Figure 4.2 Typical Hamburg Wheel Tracking Device Test Results for Center of Specimen

Table 4.1 Binder Abbreviations Used in This Study

Binder Type	Abbreviation
Wright Asphalt PG 64-22	W 64
Wright Asphalt PG 70-22 3.5% SBS	W 70 SBS
Wright Asphalt PG 76-22 SBS & TR	W 76 SBS & TR
Ultrapave PG 67-22	U 67
Ultrapave PG 76-22 3.5% SBR	U 76 SBR
Valero Armor PG 64-22	V 64
Valero Armor PG 70-22 2% Elvaloy	V 70 E
Valero Armor PG 76-22 3.5% Elvaloy	V 76 E
BASF PG 64-22	B 64
BASF PG 70-22 2% SBR	B 70

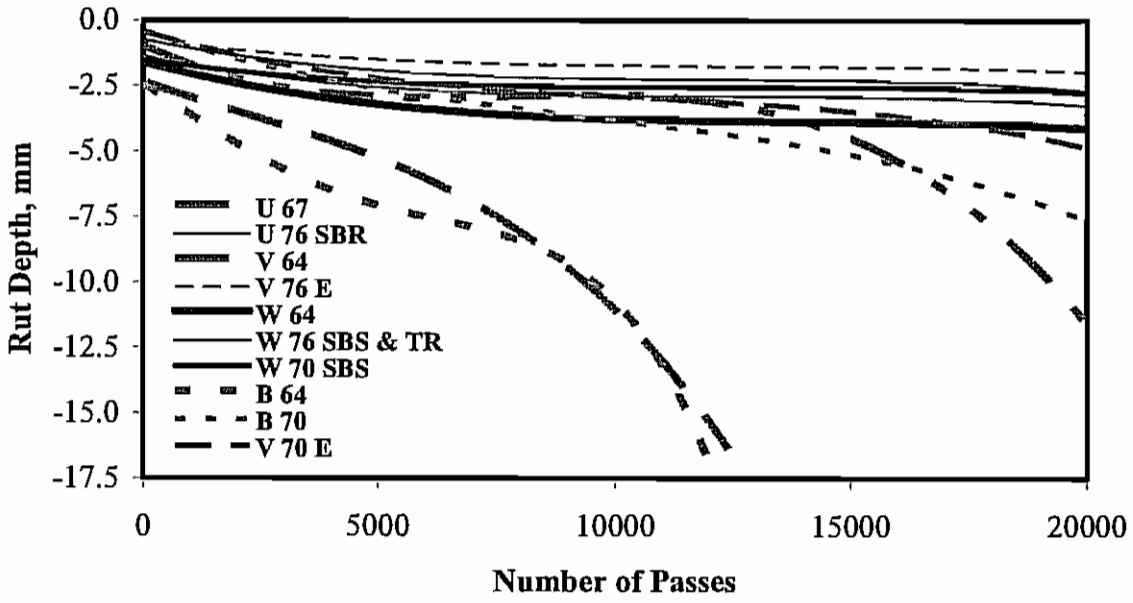

Figure 4.3 HWTD Rut Depth for Type D Mix Design at the Center of the Slab

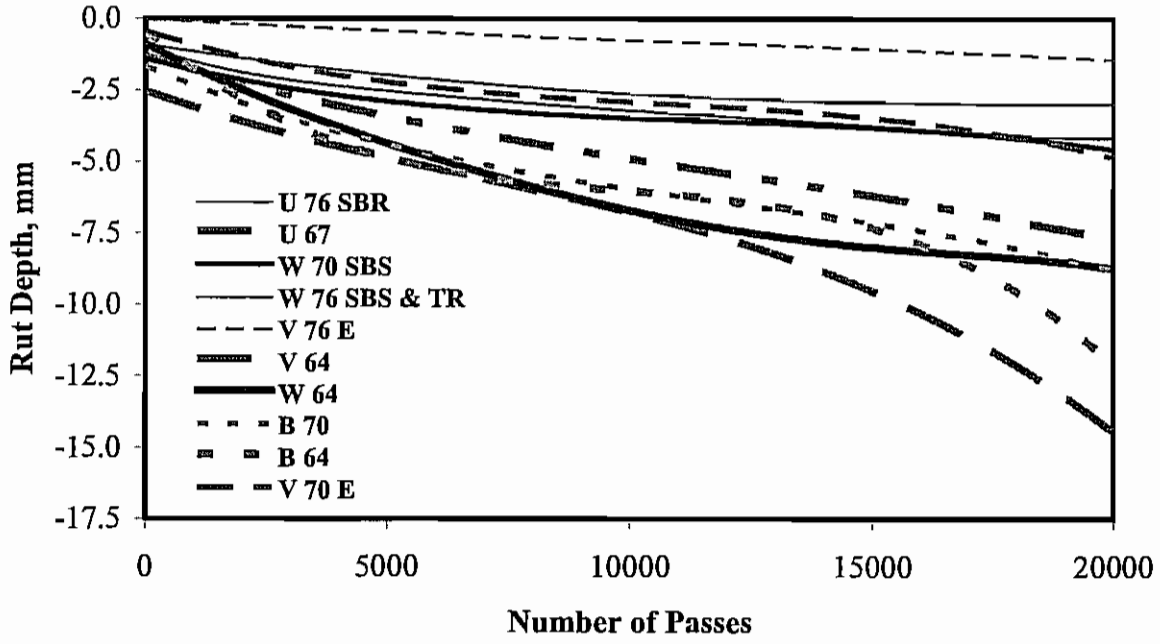

Figure 4.4 HWTD Rut Depth for CMHB-C Mix Design at the Center of the Slab

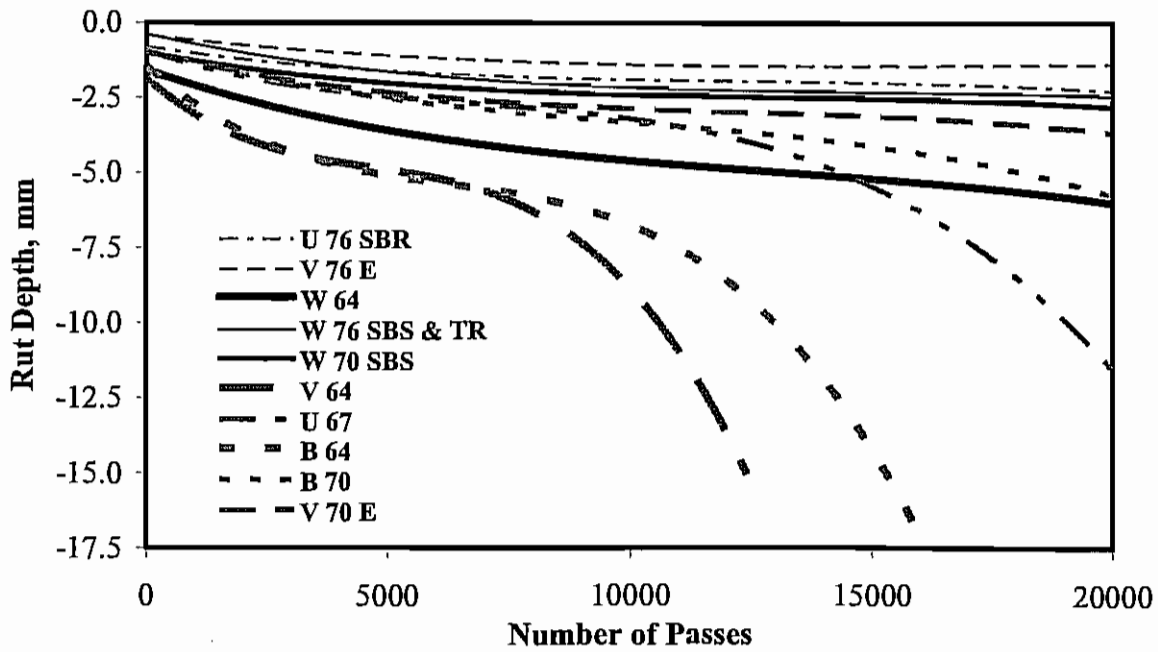

Figure 4.5 HWTD Rut Depth for Type D Mix Design at the Center of Specimen

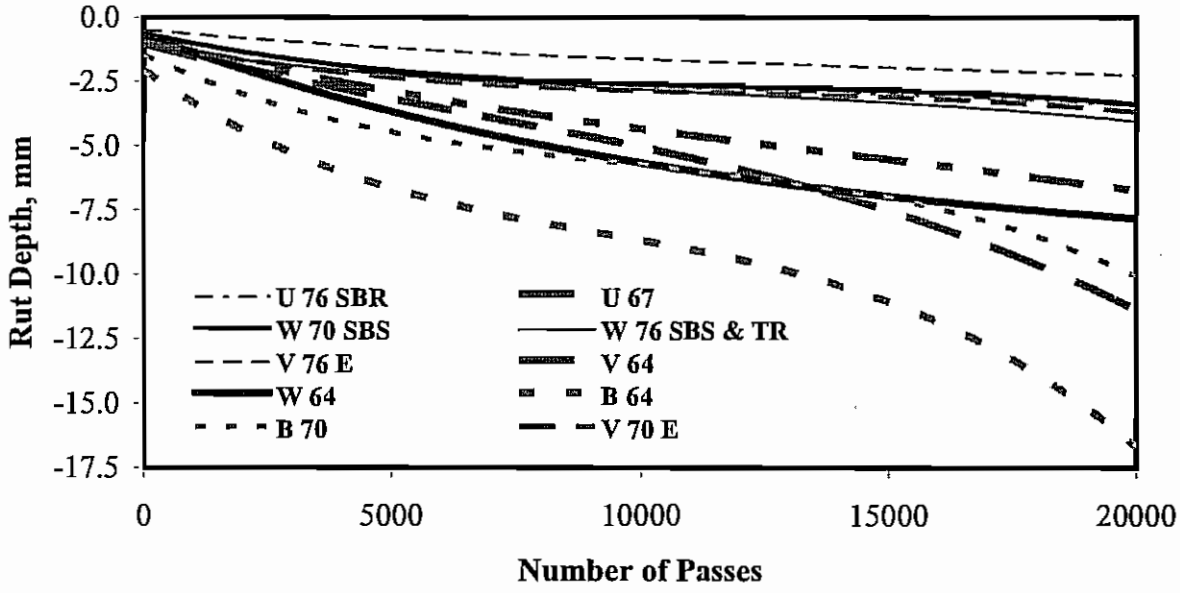

Figure 4.6 HWTD Rut Depth for CMHB-C Mix Design at the Center of Specimen

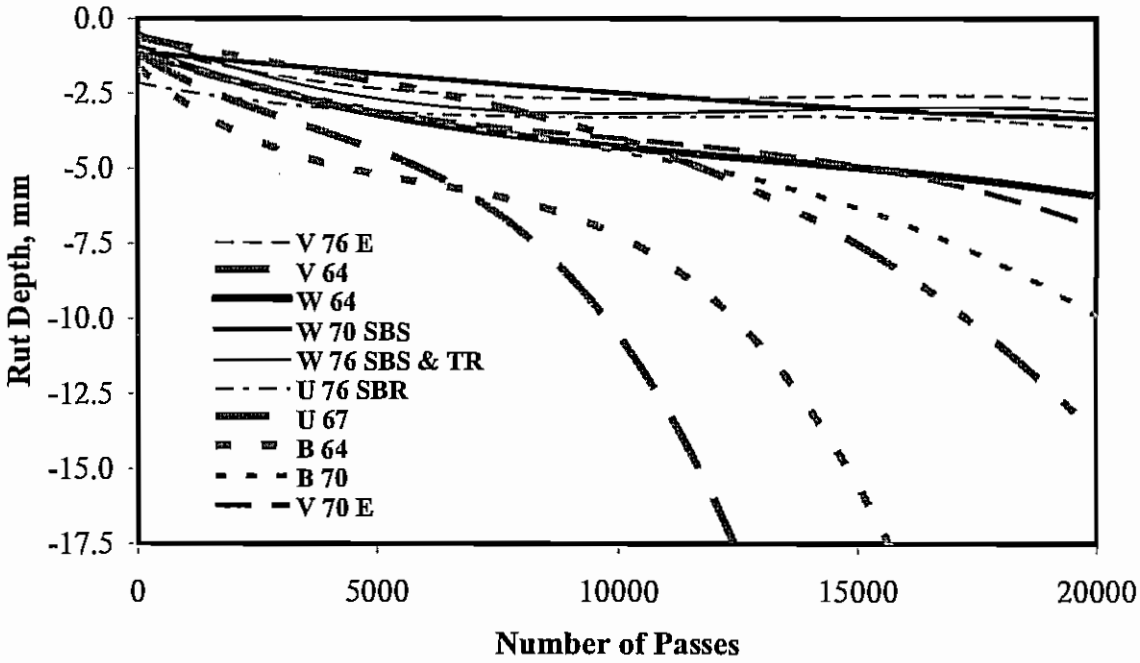

Figure 4.7 HWTD for Type D Mix Design Maximum Rut Depth

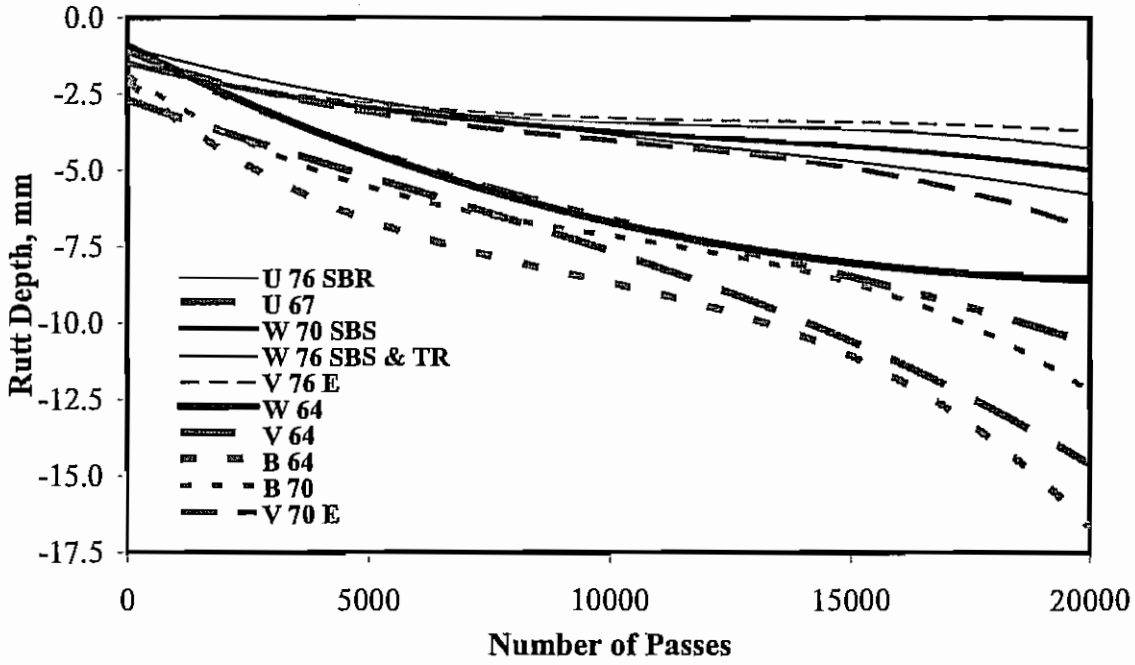

Figure 4.8 HWTD for CMHB-C Mix Design Maximum Rut Depth

Table 4.2 Rut Depth at the End of the Testing

Asphalt Type	Center of Specimen Deformation, mm		Maximum Deformation, mm		Center of Slab Deformation, mm	
	Type D	CMHB-C	Type D	CMHB-C	Type D	CMHB-C
W 64	4.0	8.0	4.4	6.1	4.0	6.1
W 70 SBS	2.9	3.4	2.8	4.9	2.7	4.6
W76 SBS & TR	2.7	4.1	3.0	5.4	2.6	4.2
V 64	14.2	9.3	17.0	12.7	16.4	12.0
V 70 E	4.7	10.6	5.4	13.0	3.9	13.0
V 76 E	2.3	2.6	2.3	3.4	1.6	2.0
U 67	9.2	7.2	14.4	11.1	13.3	7.6
U 76 SBR	2.5	3.5	3.2	3.9	2.8	3.0
B 64	17.8	15.0	17.8	16.7	17.1	16.7
B 70	10.1	9.2	11.0	9.5	7.4	8.2

For the Type D mix design, in the case of TxDOT specifications, only 3 binders exceeded the maximum 12.5 mm deformation limitation set; Ultrapave 67-22, BASF 64-22, and Valero Armor 64-22. According to TxDOT specifications (Table 2.2), all three binders need only to remain under 12.5-mm deformation until 10,000 cycles due to the fact that they have temperature grade of 64°C. Exposing

these base binders to 20,000 cycles provided a better understanding of their overall performance. In comparing Ultrapave 67-22 to Valero Armor 64-22 at 10,000 cycles, the two seem almost identical in their performance, with both deforming around 4 mm. By allowing them to endure 20,000 cycles, Valero Armor was seen to be a better binder because it only reached a deformation of 6 mm compared to the 15 mm of deformation experienced by Ultrapave. This observation could not have been made if the binders had been tested to only the 10,000 cycles specified by TxDOT for PG 64 binder. The prompt failure after 10,000 seen in the base Valero Armor binder can be attributed to moisture susceptibility of the binder (Sagi, 2004).

The base binder that performed the best overall was Wright Asphalt, followed by Ultrapave and Valero Armor. When modified, all three binders significantly reduced the deformation to 5 mm or less. The only binder that did not seem to show significant improvement with modification was the BASF binder. Before modification, the binder performed poorly and did not complete 20,000 cycles before reaching the maximum deformation of 18 mm. After modification, the binder improved but still deformed over 10 mm which is large in comparison to the other modified binders.

The amount of deformation across the specimen is higher in the center of the slab when compared to the average between the centers of the two specimens. Therefore, when using the center of specimen as an indicator of performance, the requirement for the maximum allowable deformation needs to be stricter since a smaller amount of deformation occurs in this region.

HWTD test results for CMHB-C mix design specimens show similar trends to that of the Type D mix design with only BASF 64-22 and Valero Armor 64-22 exceeding the 12.5 mm deformation limit.

Deformation values of CMHB-C mix design are slightly less than those of Type D mix in most cases. In the cases where the deformation exceeded 4 mm, the CMHB-C mix design withstood deformation better than that of the Type D mix design. This indicates that CMHB-C is a more resilient mix in comparison to the Type D mix, which is to be expected as CMHB-C mix is designed for heavier loading conditions.

4.2 DSR TEST RESULTS

The DSR tests were performed according to the procedure specified by Bahia et al. (2001) for repeated creep mode of loading and as per AASHTO T 315-04. The specimens for both test types were prepared as per AASHTO T315-04. A minimum of three specimens were tested for each mode of loading and temperature and only the average value is reported here.

4.2.1 Repeated Creep Test Results

The repeated creep tests were performed at eight stress levels (25, 50, 100, 200, 400, 800, 1,600, and 3,200 Pa) and three temperatures (52, 64, and 76 °C). A typical test result for two binder types and two stress levels (25 and 3,200 Pa) is shown in Figure 4.8. The data presented in the figure is for the tests performed at 70 °C (158 °F) for asphalts obtained from Valero Armor and Ultrapave for both modified and unmodified binders. The test results suggest that the increase in stress from 25 to 3200 Pa increased accumulated strain from 4% to 2000% at the end of the loading. In addition, the increase in accumulated strain was significantly less for asphalt modified with 3.5% Elvaloy (V76 E) even at the higher stress levels of 3200 Pa. Also, the accumulated strain levels were significantly less in the modified asphalt at both stress levels. Similar trends were observed for the remainder of the asphalt types.

In terms of the influence of stress level, the test results at the end of 100 cycles for four stress levels and three temperatures for W 76 SBS & TR are shown in Figure 4.10. The results indicate that the accumulated strains increase with increase in temperature and strain level. The increase in accumulated strain is significant from 100 to 800 Pa, but is not that significant for further increase in stress at 52 °C. However, the influence is significant when the temperature is increased from 52 to 76 °C.

Although not presented here, the repeatability of the test increased with the decrease in stress levels. However, at very low strain levels, the resolution of DSR was not adequate to discriminate between the binder types, while at very high stress levels the strain values become more erratic and not as consistent when the tests were repeated. Therefore, it was decided to evaluate the data at 100 Pa. The test results for unaged binder at 100 Pa for the three temperatures is shown in Figure 4.11. The data suggests that increase in temperature increases accumulated strain and increase in strain with temperature is non-linear. In general, the modified binders exhibited less deformation in comparison to unmodified binders.

The test results also suggest that BASF asphalt binder had maximum accumulated strains while Wright Asphalt modified with SBS and TR had minimal accumulated strains. In addition, some asphalt binders exhibited higher increase in strains in comparison to the others. For instance, Valero Armor asphalt with 3.5% Elvaloy exhibited lower accumulated strains at 52 °C in comparison to Wright Asphalt modified with SBS and TR, but exhibited higher accumulated strains at 76 °C indicating that accumulated strain levels are non-linearly dependent on temperature.

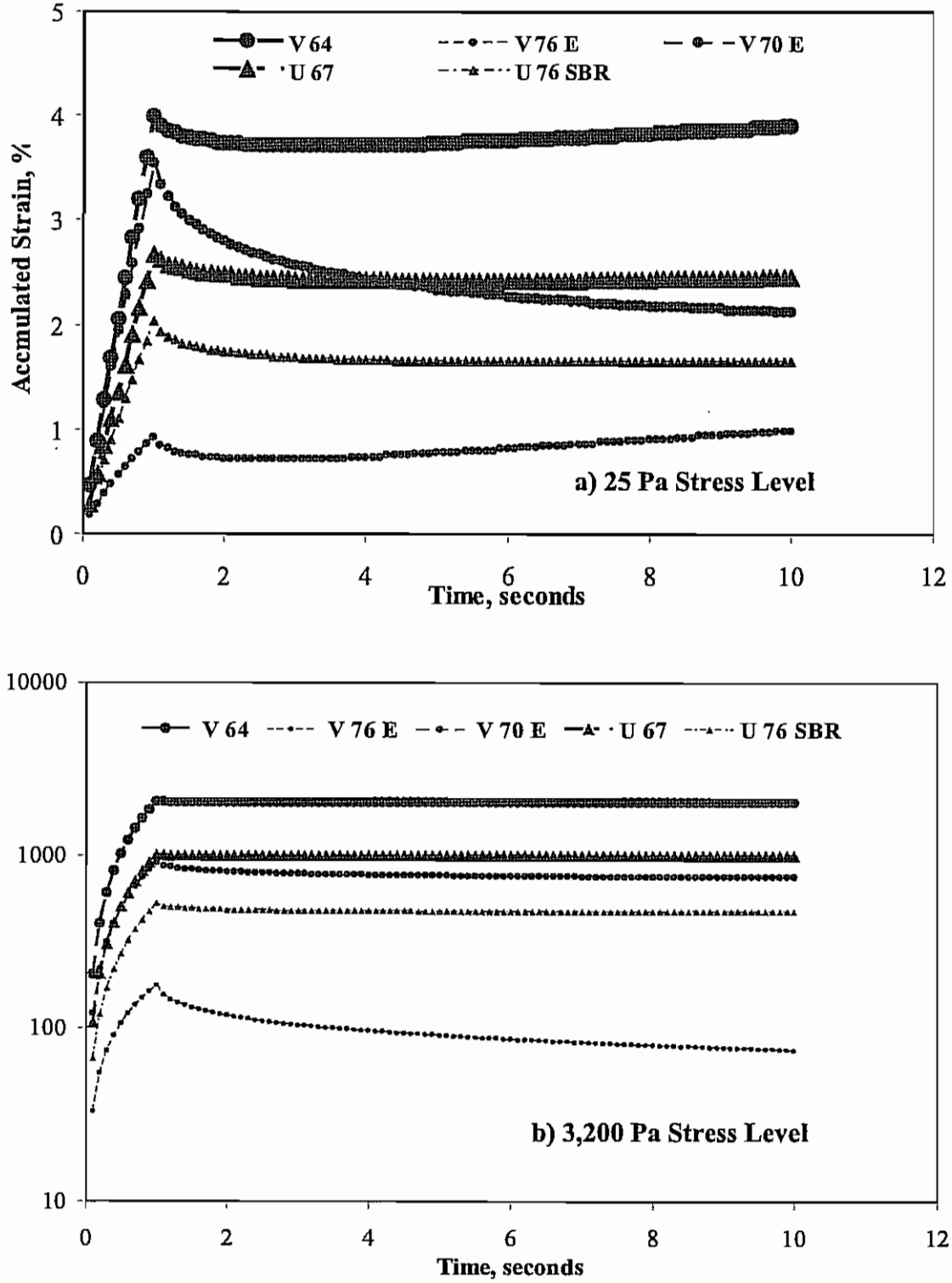

Figure 4.9 Typical Repeated Test Results at 70 °C at the end of First Cycle

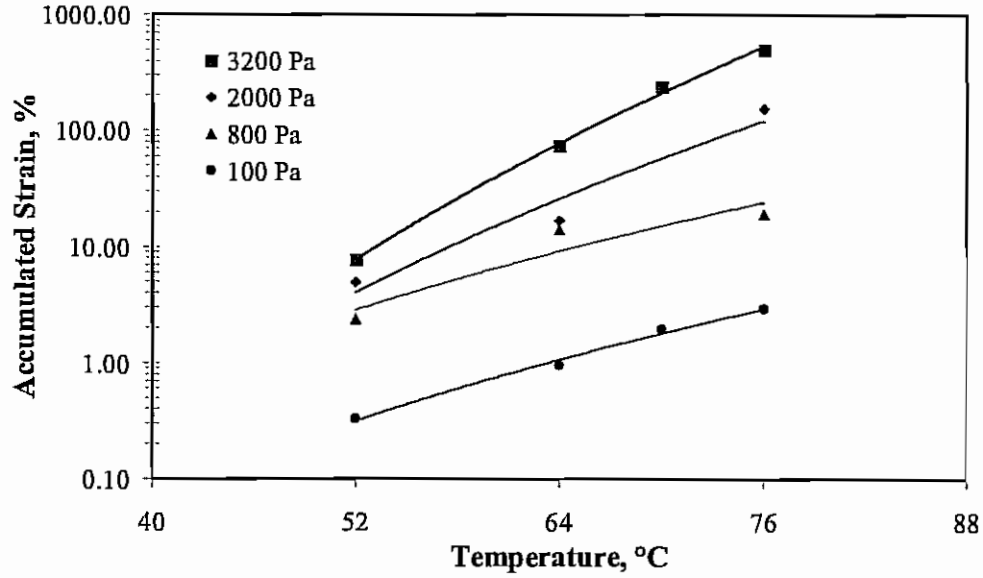

Figure 4.10 Accumulated Strain at a Shear Stress of 100 Pa After 100 Creep and Recovery Cycles

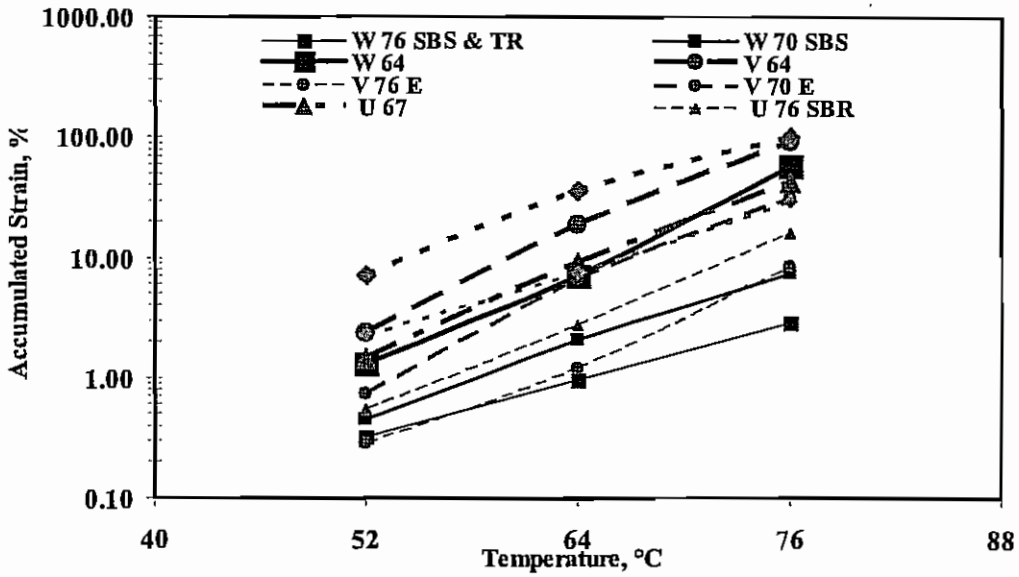

Figure 4.11 Accumulated Strain at a Shear Stress of 100 Pa at the end of the Test for Unaged Binder

For comparing accumulated strains of aged and unaged binders, the strain data is summarized in Table 4.3. The data suggest that the RTFO aged binder generally exhibited more accumulated strains even though they are expected to be stiffer in comparison to unaged binders. However, in some cases the RTFO aged binder exhibited lower accumulated strains. For example, Wright Asphalt consisting of SBS has accumulated strains of 0.449% for unaged binder but only 0.357% accumulated strains were observed for RTFO aged binders at 52 °C. The data presented in Table 4.3 also suggest that the binder ranking (based on accumulated strains) can change with change in test temperatures. For example, Valero Armor asphalt binder with 2.0% Elvaloy (V 70 E) had the lowest accumulated strains at 52 °C but Wright Asphalt with SBS and TR (W 76 SBS and TR) had the lowest accumulated strains at 76 °C. However, the test results clearly indicate that the asphalts with modifiers have significantly lower accumulated strains in comparison to unmodified asphalt binders.

Table 4.3 Accumulated Strain Obtained from Repeated Creep Test at 100 Pa

Asphalt Type	Accumulated Strain, %					
	52 °C		64 °C		76 °C	
	Unaged	RTFO	Unaged	RTFO	Unaged	RTFO
W 64	1.312	2.427	6.968	16.380	57.637	81.250
W 70 SBS	0.449	0.357	1.562	1.493	7.414	9.413
W76 SBS & TR	0.325	0.495	0.954	1.163	2.895	4.859
V 64	2.336	3.504	18.677	19.900	91.474	117.300
V 70 E	0.730	1.828	6.587	6.641	31.488	41.170
V 76 E	0.282	0.610	1.190	2.085	8.503	15.670
U 67	1.448	1.474	9.054	8.333	42.753	42.290
U 76 SBR	0.546	0.545	2.754	3.118	15.945	15.530
B 64	7.009	6.297	36.121	37.470	101.221	155.200
B 70	2.830	3.702	7.489	17.710	29.214	88.390

In addition, the order of magnitude of accumulated strain corresponds to the temperature grade. For instance, the accumulated strains obtained for RTFO aged Valero Armor PG 64-22 asphalt binder is around 20% while for PG 76-22 asphalt binder from the same source is 16%, which indicates that PG 76-22 grade asphalt has similar levels of accumulated strains to that of PG 64-22 asphalt binder at their corresponding test temperatures. Overall, the data suggest that the repeated creep tests be performed at temperatures corresponding to at least one or two PG grades higher to better differentiate between binders consisting of modifiers.

4.2.2 *Frequency Sweep Test Results*

The frequency sweep tests were also performed at 52, 64 and 76 °C with frequencies varying from 0.01 to 24.1 Hertz with measurements taken at 20 different intervals between the two frequencies. Again, the tests were performed on three specimens and the average value is presented in this study. A typical test result for Wright Asphalt PG 64-22 at three temperatures is shown in Figure 4.12. The measured complex modulus increased with decrease in temperature. The complex modulus (G*) data was shifted horizontally to develop a master curve at a reference temperature of 64 °C using time temperature superposition principle (Pagen, 1963) and is shown in Figure 4.13. The developed master curve was divided by and multiplied by sin δ in order to differentiate between modified and unmodified asphalts. The data for base asphalts (PG 64-22 or PG67-22) and modified asphalts (PG76-22) are shown in figures 4.14 and 4.15, respectively. The data for G*/sinδ and G*x sinδ is shown with solid and hollow symbols, respectively.

The data presented in the figures indicates that the aged asphalt binder exhibited higher values compared to unaged binder for both parameters (G*/sinδ and G*x sinδ). However, the summarized data indicates that influence of modifier is not as evident as from repeated creep test (Figure 4.16). For instance, a maximum G*/sinδ value of 220 kPa is observed for aged base asphalt binder and 222 kPa is observed for aged modified asphalt binder (Wright Asphalt). The data presented in Figure 4.16 suggests that the presence of modifier can only be identified at the frequencies less than 0.5 Hz while SHRP specifications suggest testing to be performed at 1.59 Hz. Such results indicate that the test is not successful in differentiating between modified and unmodified asphalt binders, which has been observed by other researchers (Bahia et al., 2001; Marasteanu, et al., 2005).

Since the typical analysis is performed at 1.59 Hz, the G*/sinδ values were plotted at the different temperatures at this frequency to further evaluate the parameters' ability to discriminate between modified and unmodified binders. The relationships between G*/sinδ and temperatures for aged and unaged binders are shown in Figures 4.17 and 4.18, respectively.

All of the binders behaved similarly before aging, with Wright Asphalt 76-22 and 70-22 behaving slightly better than the other binders. When the binders were aged they began to exhibit different trends. A trend similar to the accumulated strain and HWTD deformation was noticed in that the BASF unmodified binder showed the least rut resistance, followed by the modified BASF and base Valero Armor. As with the accumulated strain and HWTD data, Wright Asphalt and Ultrapave with modification proved to have the highest rut resistance yielding the highest G*/sinδ values. However, the G*/sinδ values were not able to differentiate between different types of modifiers especially at frequencies of 0.5 Hz or higher.

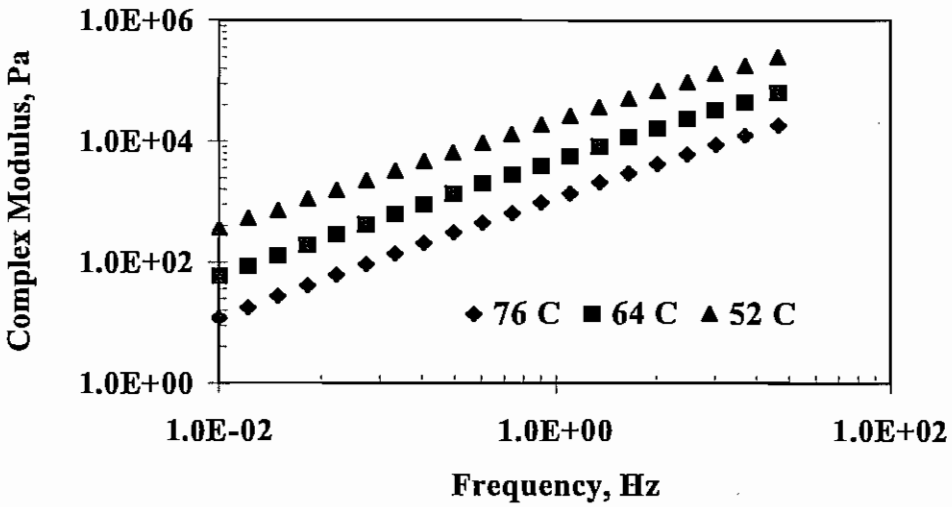

Figure 4.12 G* vs. Temperature Relationship for Wright Asphalt (W 64)

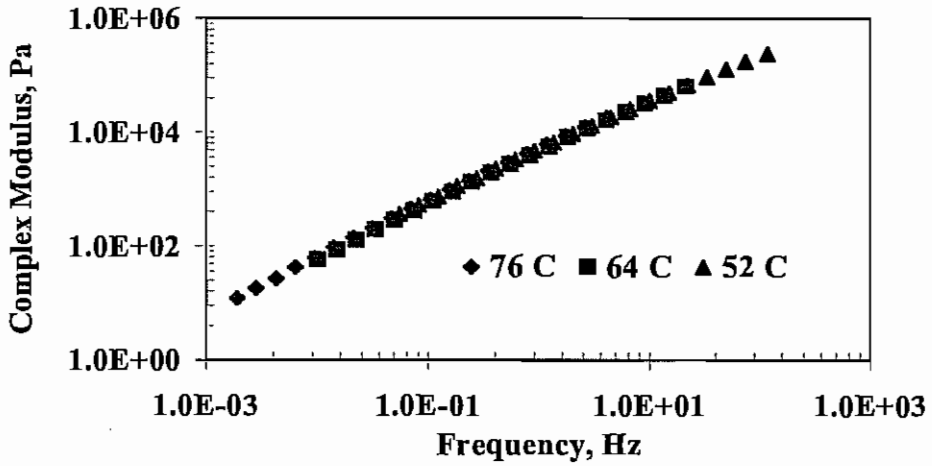

Figure 4.13 G* vs. Temperature Relationship for Wright Asphalt (W 64) at 64 °C

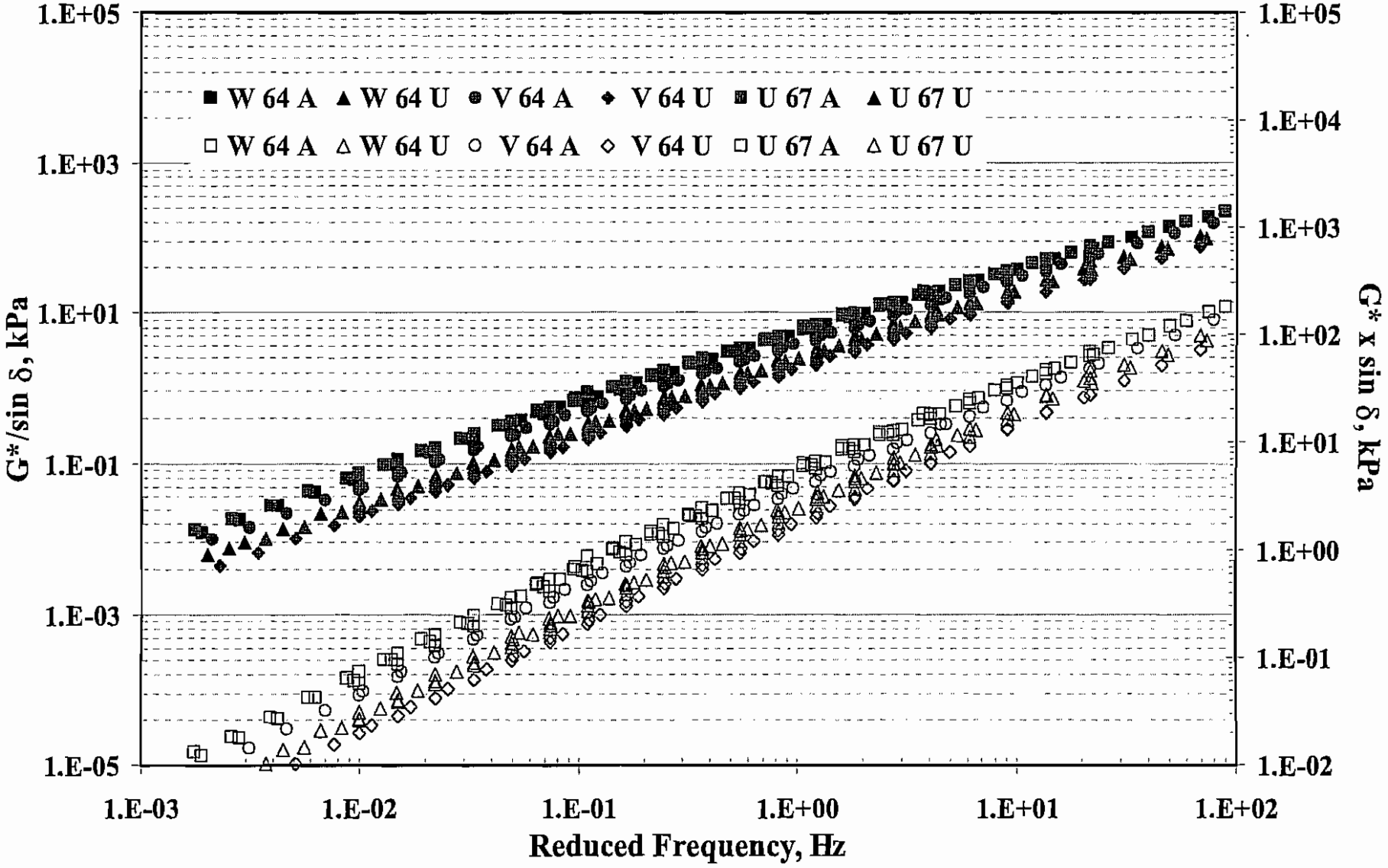

Figure 4.14 G*/sinδ and G*x sinδ Values for Base Binders

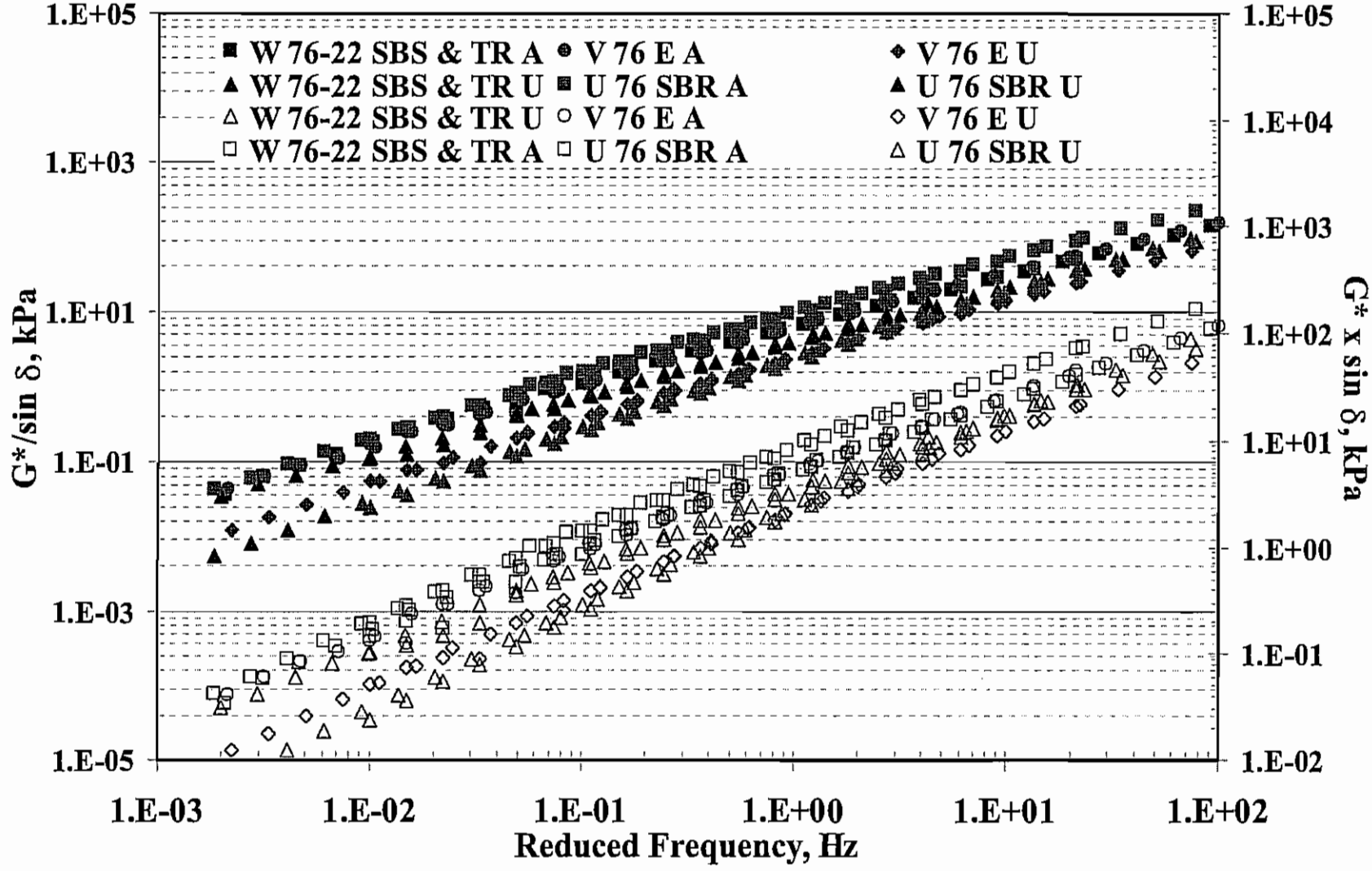

Figure 4.15 G*/sinδ and G*x sinδ Values for Modified Binders

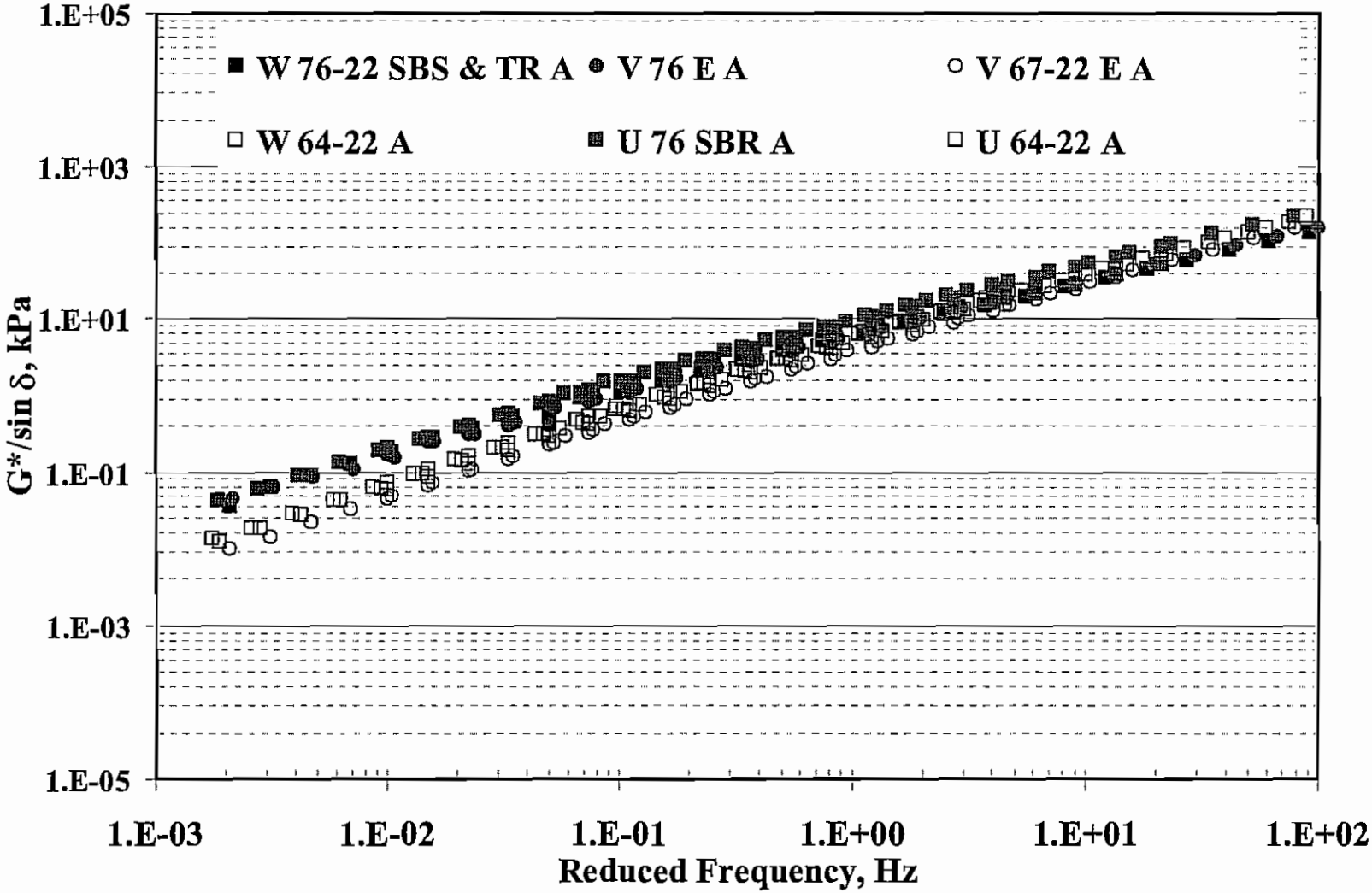

Figure 4.16 G*/sinδ Values for Base and Modified Binders

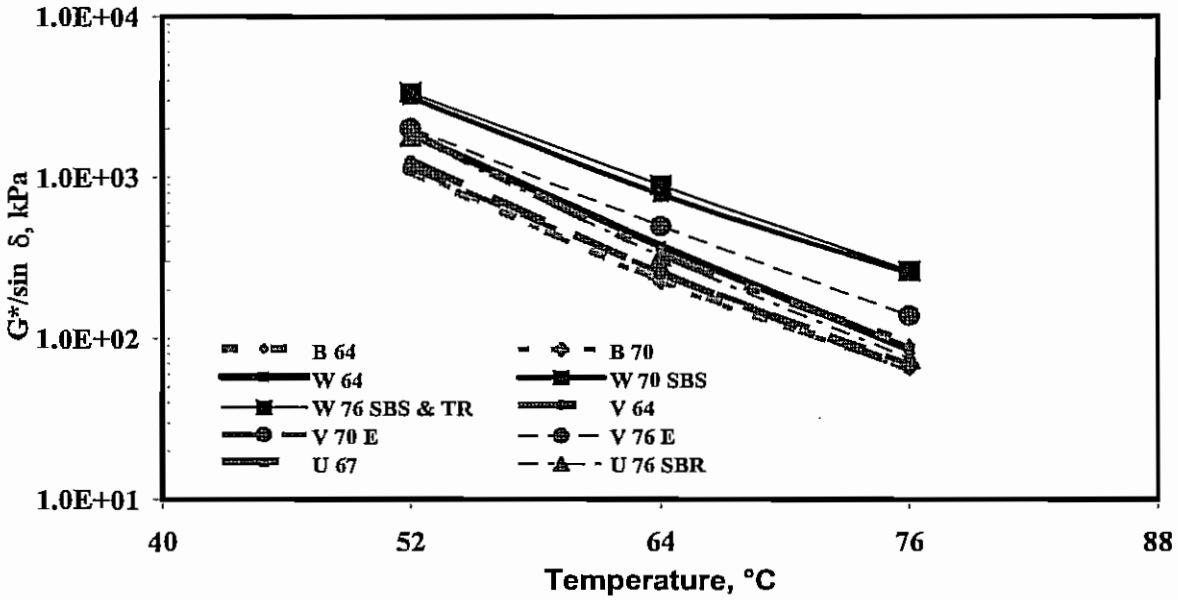

Figure 4.17 G*/sinδ vs. Temperature for All Unaged Binders

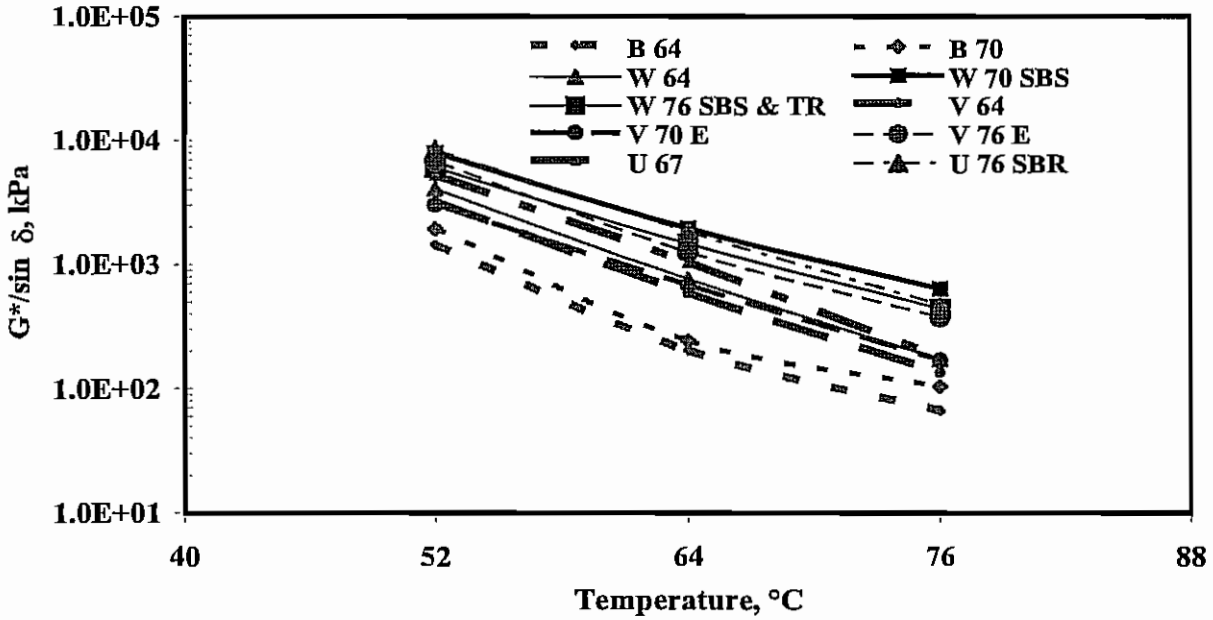

Figure 4.18 G*/sinδ vs. Temperature for All RTFO Aged Binders

4.3 COMPARISON

By maintaining all parameters constant, i.e. air voids, aggregate type, mix design, and testing temperature, and only altering the binder type, it is possible to identify the influence of binder type on the rut depth measured using HWTD. Therefore, an attempt was made to identify the relationship between measured binder and HMAC properties, and the results are presented in the following sections.

4.3.1 Correlation Between G/sinδ and Accumulated Strain*

Since G*/sinδ and accumulated strain identify rutting potential of the binder, it was decided to develop a correlation between the two measured parameters. An existence of non-linear relationship was identified and is presented in Figure 4.19. The data suggests that the relationships are dependent on temperature as well as aging of asphalt binder. The coefficient of determination (R^2) value was highest at 52 °C (0.89) followed by 76 °C (0.80) and the lowest was found to be at 64 °C (0.78) for unaged binder. However, the R^2 value for aged asphalt binder dropped significantly and the maximum value of only 0.71 was found at 76 °C. Since rutting potential of HMAC will be based on the performance of aged binders at 50 °C, the G*/sinδ value may not be well correlated to the rut depth measured using HMAC. However, further evaluation is needed before a definite conclusion can be drawn.

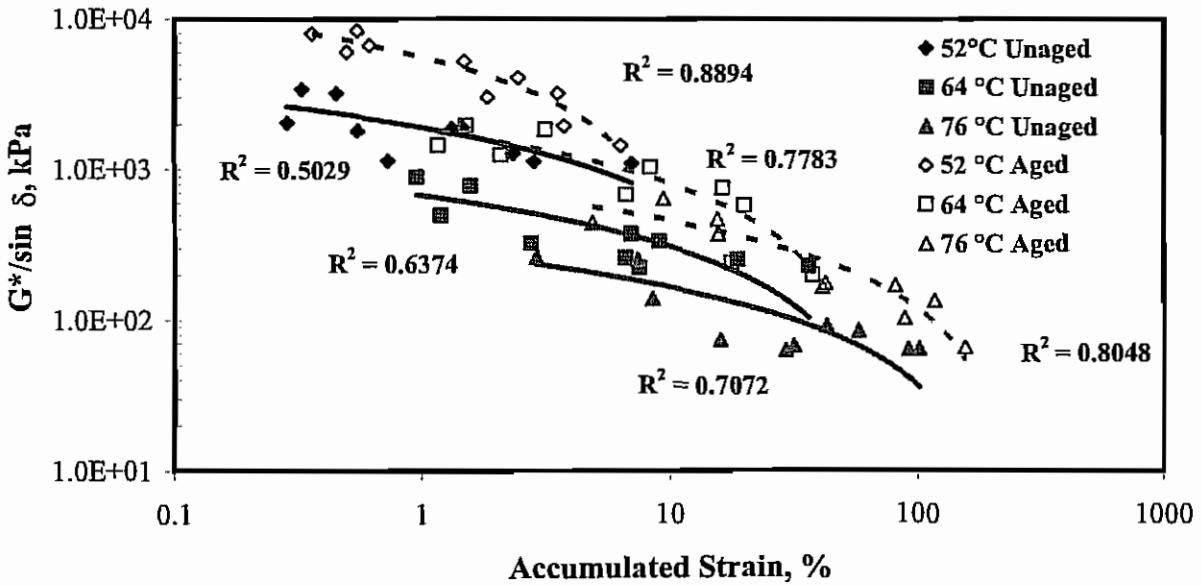

Figure 4.19 G*/sinδ vs. Accumulated Strain for All Binder Types

4.3.2 Relationship between G/sinδ and HWTD Rut Depth*

The relationship between rut depth at center of specimen, center of slab and maximum deformation versus G*/sinδ measured on aged binder is presented in Figures 4.20 to 4.22. It is expected that an increase in temperature causes a decrease in the G*/sinδ which in turn should cause a decrease in the rut resistance of the HMAC. The data in the figure suggests that a decrease in G*/sinδ value increases the observed deformation of the HMAC specimens at the specific temperature. However, the drop in measured G*/sinδ value from one temperature to another one did not change the deformation measured using HWTD. The reason for this discrepancy is that HWTD tests were only performed at 50 °C.

The data presented in Figure 4.20 suggests that the 76 °C G*/sinδ values correlate well with center of specimen deformations. The R^2 values are more than 0.7 indicating stronger correlation between the two parameters. However, the correlation reduced significantly at lower temperatures. Typically, it would be expected that G*/sin δ should be correlated well at 52 °C because it is close to the HWTD test temperature. The test results also suggest that the stronger correlations exist with CMHB-C mixes in comparison to Type D mixes for three temperatures. The data presented in Figures 4.21 and 4.22 show similar trends accept that the R^2 values are significantly lower.

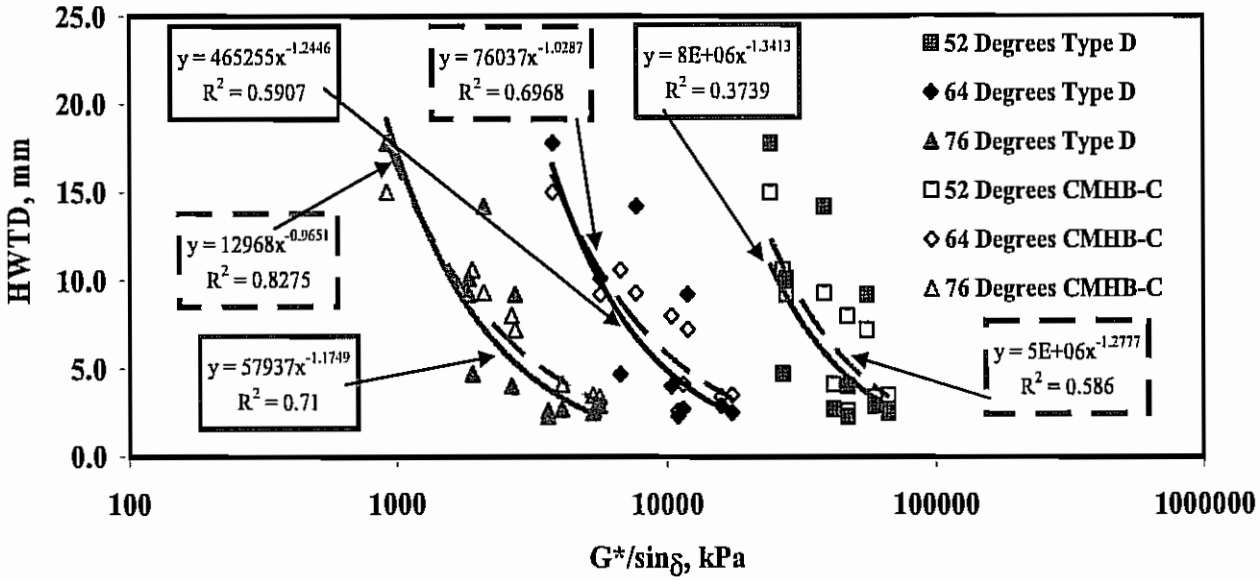

Figure 4.20 G*/sinδ vs. Rut Depth at Center of Specimen from HWTD for All Binder Types

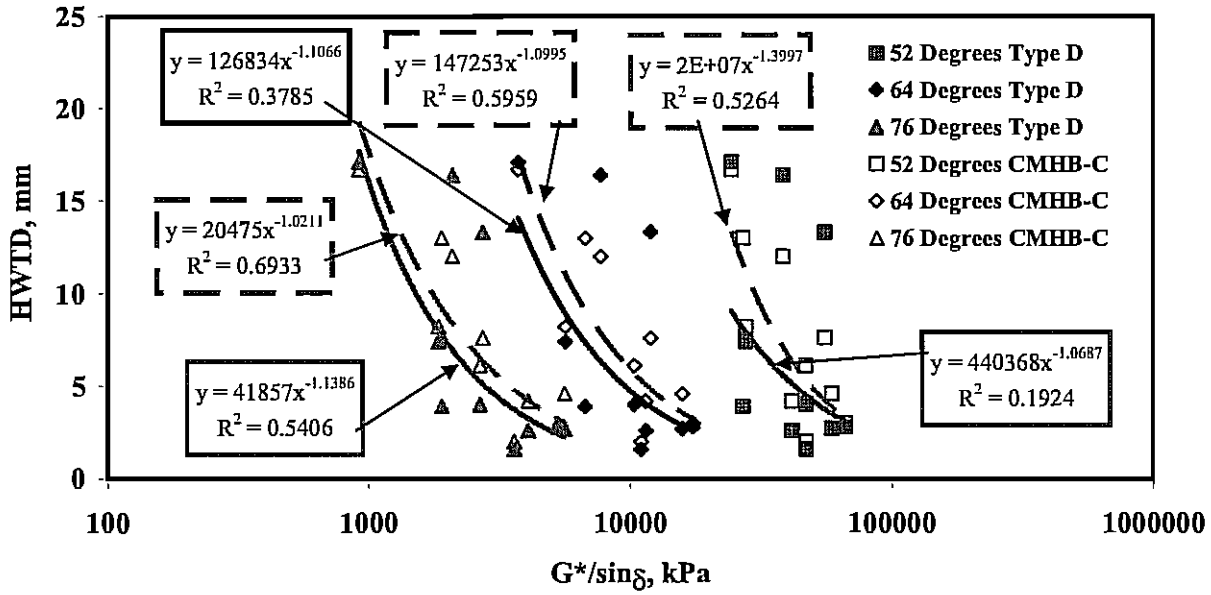

Figure 4.21 G*/sinδ vs. Rut Depth at Center of Slab from HWTD for All Binder Types

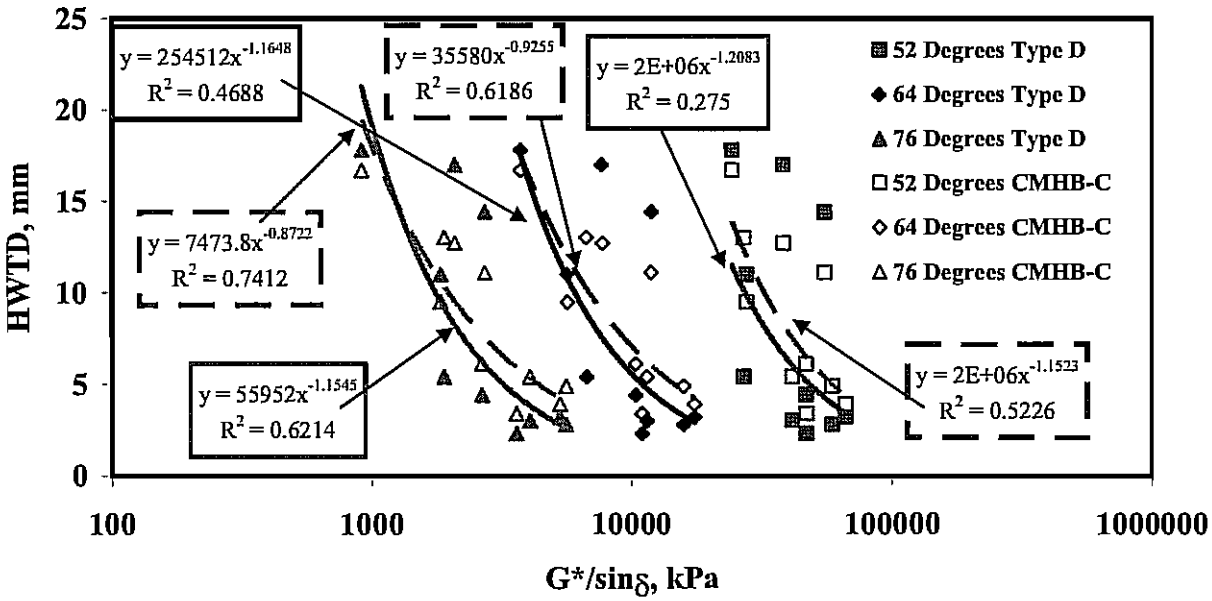

Figure 4.22 G*/sinδ vs. Rut Depth at Maximum from HWTD for All Binder Types

The data presented in the figures suggest that the best correlation exists between G*/sinδ at a test temperature of 76 °C and rut depth measured at the center of the specimens. Although the correlation exists, the standard error (Section 4.3.42) is higher by more than 100 for all the temperatures, indicating that the correlation does not clearly explain the relationship between the two. Overall, the relationship between G*/sinδ and HWTD rut depth seems to be a weak relationship.

4.3.3 Correlation of Accumulated Strain to HWTD Rut Depth

The accumulated strain from repeated creep test and rut depth results obtained from three HWTD test locations are summarized in Table 4.4 for all binder and mix types. To develop a correlation, the data obtained from the two tests was plotted and a linear regression line was fitted to the data. A typical example of the relationship between accumulated strain and rut depth (at the center of the specimen) is shown in Figure 4.23 for unaged binder. The data presented in Figure 4.23 suggests that a correlation between the two exists, as R^2 is more than 0.70. However, the correlation between the deformation and accumulated strain became progressively weaker when a comparison to center of slab and maximum deformation was made (Table 4.4). Mix designs Type D and CMHB-C were correlated separately and then combined to view all the possibilities of different relationships.

This analysis was also performed using the deformation found at the center of slab and maximum deformation, and can be seen in Figures 4.24 and 4.25, respectively. Mix designs Type D and CMHB-C were plotted separately and then combined to view all the possibilities of different relationships. Since the correlation was seen as somewhat weak using the unaged binder for DSR testing, it was decided to identify relationships using aged binder. By aging the binder, conditions were achieved that are closer to those seen in the HWTD test and the actual field conditions, since the binders in both of those conditions were short term aged. The sample specimens were placed in the oven before compaction and the field material was transferred to the site location from the plant, thus experiencing short term aging during transportation.

By comparing RFTO aged binder accumulated strain to the same HWTD rut depth, a stronger correlation was observed than that of the unaged binders as shown in Figures 4.26 through 4.28. The data shows that the R^2 values typically increased by 0.1 or higher, indicating that the correlation is better with RTFO aged binder than unaged binder. The relationship between Type D, CMHB-C and the combination of the two data sets was also performed. Since the strongest correlation was seen at 52 °C at the center of the specimen, it was decided to pursue this relationship.

Table 4.4 DSR Accumulated Strain and HWTD Rut Depth Data

Asphalt Type	Accumulated Strain, %						Deformation at Center of Specimen, mm		Maximum Deformation, mm		Deformation at Center of Slab, mm	
	52 °C		64 °C		76 °C							
	Unaged	RTFO	Unaged	RTFO	Unaged	RTFO	Type D	CMHB-C	Type D	CMHB-C	Type D	CMHB-C
Wright Asphalt 64-22	1.312	2.427	6.968	16.380	57.637	81.250	4.0	8.0	4.4	6.1	4	6.1
Wright Asphalt 70-22 (3.5% SBS)	0.449	0.3565	1.562	1.493	7.414	9.413	2.9	3.4	2.8	4.9	2.7	4.6
Wright Asphalt 76-22 (SBS + TR)	0.325	0.4946	0.954	1.163	2.895	4.859	2.7	4.1	3	5.4	2.6	4.2
Valero Armore 64-22	2.336	3.504	18.677	19.900	91.474	117.300	14.2	9.3	17	12.7	16.4	12
Valero 70-22 (2% Elvaloy)	0.728	1.828	6.587	6.641	31.488	41.170	4.7	10.6	5.4	13	3.9	13
Valero 76-22 (3.5% Elvaloy)	0.282	0.6104	1.190	2.085	8.503	15.670	2.3	2.6	2.3	3.4	1.6	2
Ultra Base (67-22)	1.448	1.474	9.054	8.333	42.753	42.290	9.2	7.2	14.4	11.1	13.3	7.6
Ultra 76-22 (3.5% SBR)	0.546	0.5449	2.754	3.118	15.945	15.530	2.5	3.5	3.2	3.9	2.8	3
BASF 64-22 (0% SBR)	7.009	6.297	36.121	37.470	101.221	155.200	17.8	15.0	17.8	16.7	17.1	16.7
BASF 70-22 (2% SBR)	2.83	3.702	7.489	17.710	29.214	88.390	10.1	9.2	11	9.5	7.4	8.2

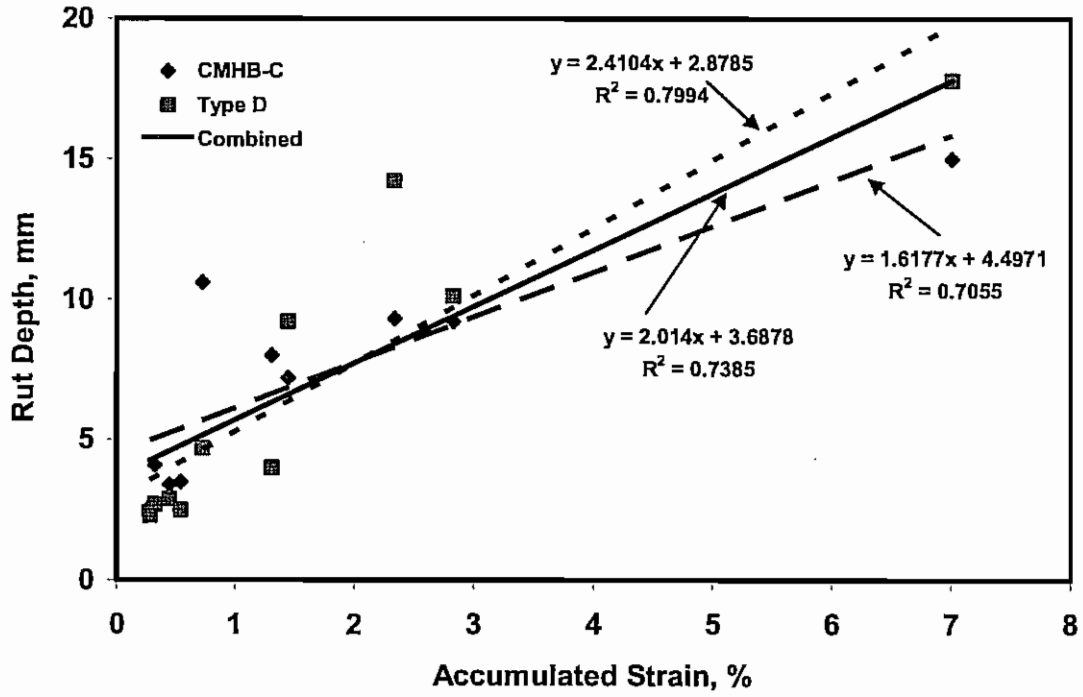

Figure 4.23 HWTD Deformation at Center of Specimen vs. Accumulated Strain of Unaged Binder at 52 °C

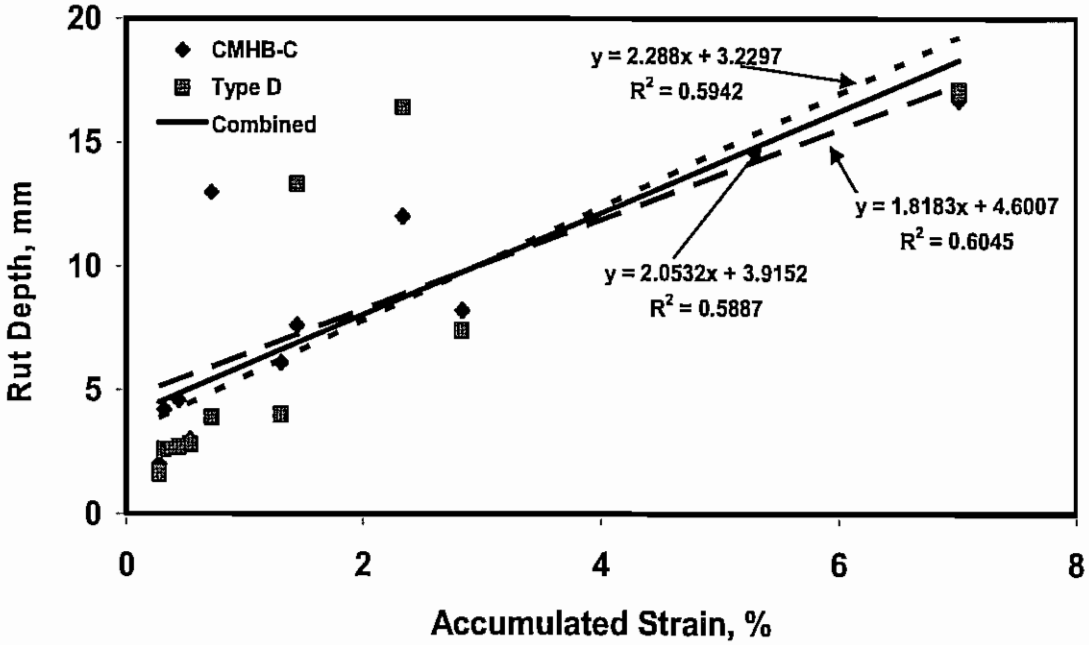

Figure 4.24 HWTD Deformation at Center of Slab vs. Accumulated Strain of Unaged Binder at 52 °C

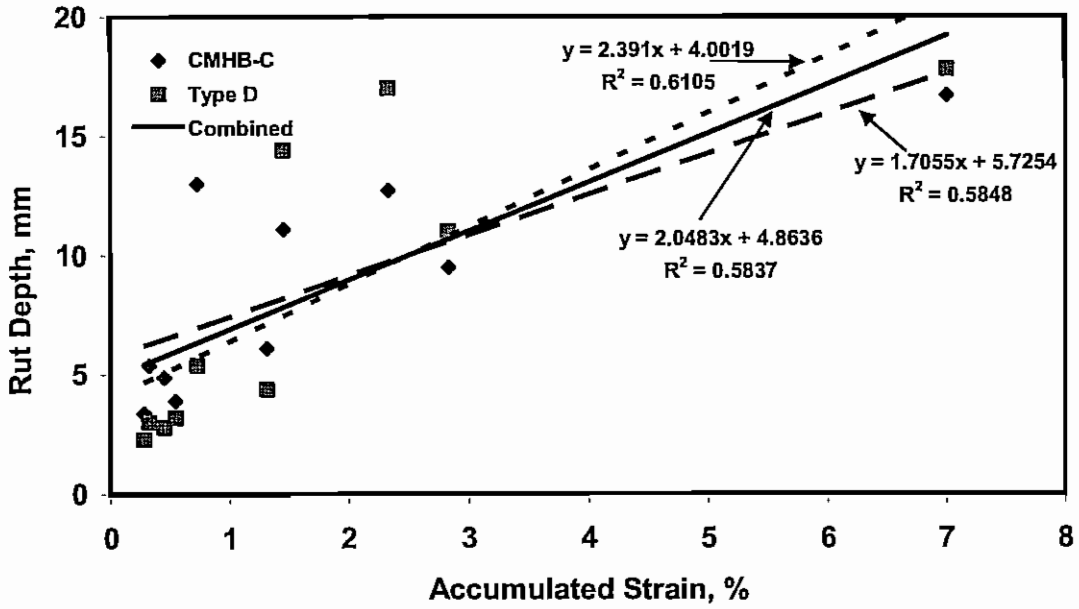

Figure 4.25 HWTD Maximum Deformation vs. Accumulated Strain of Unaged Binder at 52 °C

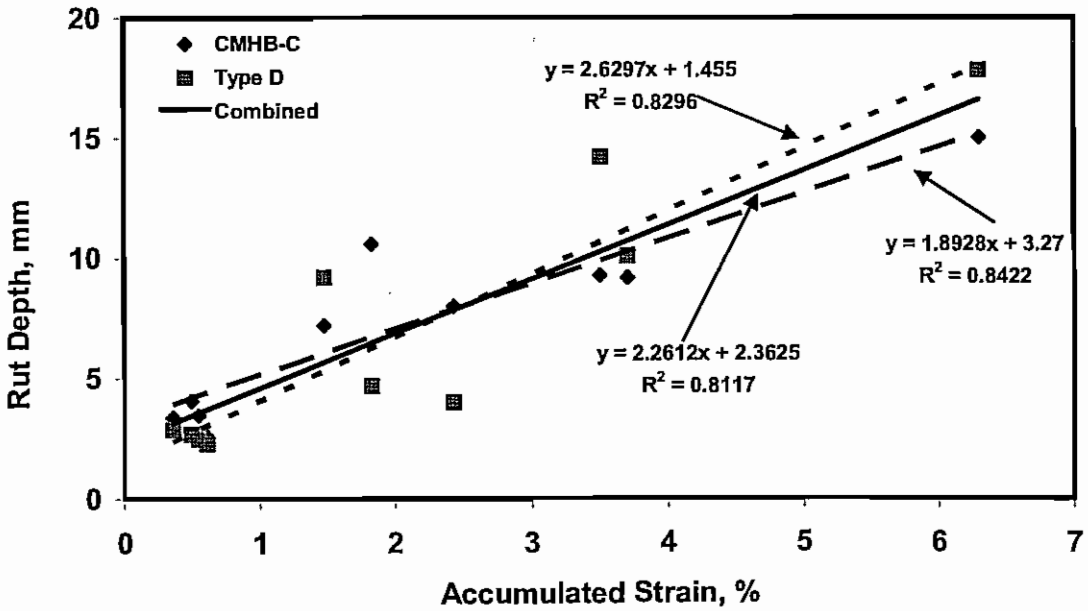

Figure 4.26 HWTD Center of Specimen Deformation vs. Accumulated Strain of RTFO Aged Binders at 52 °C

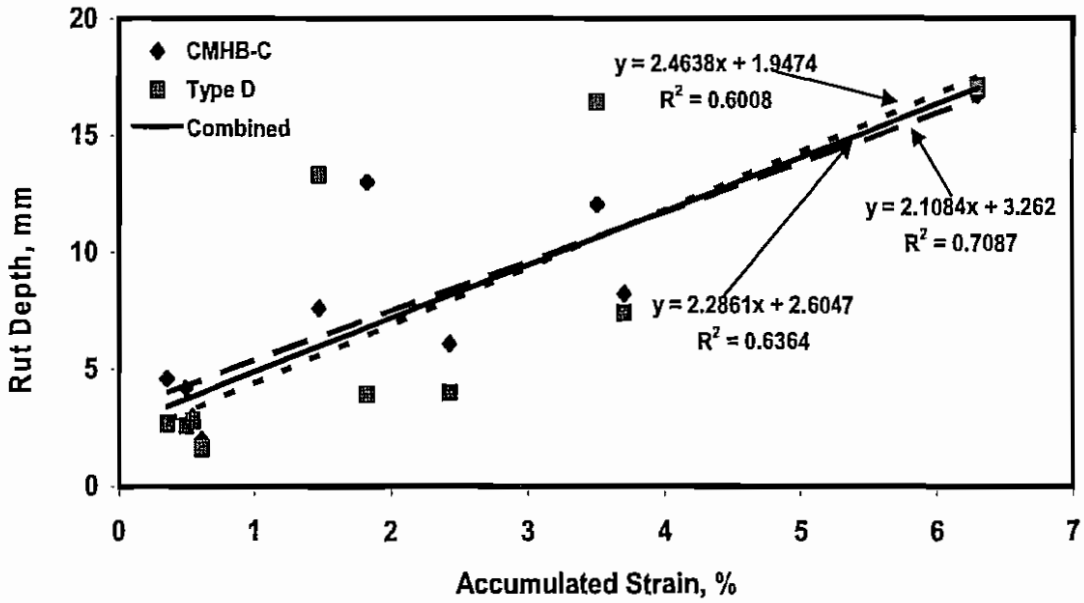

Figure 4.27 HWTD Center of Slab Deformation vs. Acc. Strain of RTFO Aged Binders at 52 °C

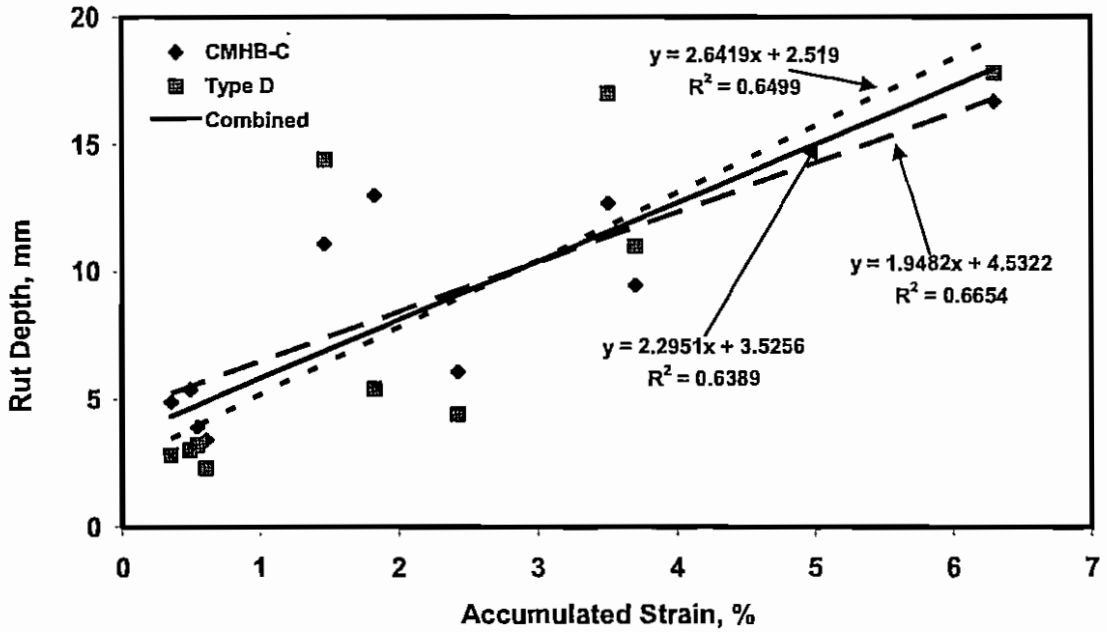

Figure 4.28 HWTD Maximum Deformation vs. Accumulated Strain of RTFO Aged Binders at 52 °C

By further interpreting the accumulated strain at 52 °C and HWTD measured rut depth at the center of specimen (Figure 4.26), an identification of binder modification can be seen. The binders yielding RTFO aged accumulated strains of less than 1% are identified as modified binders with a high temperature performance grade at or near 76 °C. A general assessment can be made that if the accumulated strain of the RTFO aged binder at 52 °C is less than 1%, a modifier is present. If this binder is used with a Type D or CMHB-C mix design, a minimal rut (< 5mm) depth can be expected in HMAC specimens provided HMAC meets specified volumetric. Any RTFO aged binder tested at 52 °C with an accumulated strain greater than 2.5% is considered to be an unmodified binder, PG 64, or a binder containing a poor modifier likely to have weak rut resistance. If this binder is used with a Type D or CMHB-C mix design, high deformation (> 10mm) of HMAC should be anticipated.

4.3.4 Validation of Relationships between DSR and HWTD Test Results

The previous section recognized a correlation between the DSR and the rut depth deformation (at the center of specimen) from the HWTD. Since linear regression is developed from a known set of data, the R^2 value is higher and may reduce significantly for an unknown set of data. In other words, the validity of this relationship needs to be further explored. Therefore, the next step in the correlation process is to validate and check the accuracy of the proposed relationship. To validate the relationship, two techniques could be employed: Data Splitting and Prediction Sum of Squares.

In Data Splitting, the original data is split into two separate sets with the first set being used to develop the model and the second to evaluate the analytical capability of the model. Data splitting should be used when $N \geq 2p + 25$, where N is the number of data points and p is the number of coefficients to be estimated (Tandon, 1994). This technique is not suitable for the current set of data because the data set does not meet the recommended number of data points.

The Prediction Sum of Squares (PRESS) technique was then chosen since the data set is small. PRESS is a variation of the data splitting technique to evaluate the precision of a model used for performance prediction (Tandon, 1994). In this procedure, one data point in the data set is removed leaving the remaining data points to develop a relationship, which is then used to predict the point that was removed. The process is then repeated by removing the next data point in the data set. The differences over the entire data set are input into Equation 4.1 to determine the PRESS R^2 value of the model.

$$R^2 = \frac{\Sigma\left[Y - \overline{Y}\right]^2 - \Sigma\left[Y - \hat{Y}\right]^2}{\Sigma\left[Y - \overline{Y}\right]^2} \qquad \text{(Equation 4.1)}$$

where:

Y = observed response for the i^{th} data point

$\overline{Y}$ = average of all the responses except the i^{th} data point

$\hat{Y}$ = predicted response for the i^{th} data point

Models with high R^2 values are considered to have small errors and are therefore classified as good models. The degree of closeness between the PRESS R^2 value and the R^2 value found by using the whole data set is a measure of the model's analytical ability. Good models will have R^2 values from the PRESS procedure close to the R^2 values from the full model (Tandon, 1994). The R^2 value found by the PRESS procedure will always be smaller than that of the R^2 value found from the complete data set. This is due to the fact that the PRESS uses fewer data points than the graphical model, which uses the complete data set.

Calculation of the standard error, $S_{x,y}$, of the data sets measures the amount of error in the prediction of y for an individual x, which allows for determining which measurement is the most accurate. Standard Error calculations are made using the given x and y variables and inputting them into Equation 4.2.

$$S_{x,y} = \sqrt{\left[\frac{1}{n(n-2)}\right]\left[n\Sigma y^2 - (\Sigma y)^2 - \frac{[n\Sigma xy - (\Sigma x)(\Sigma y)]^2}{n\Sigma x^2 - (\Sigma x)^2}\right]} \quad \text{(Equation 4.2)}$$

where:

n = the number of known x or y values
y = the known y value
x = the known x value

4.3.4.1 Validation of Relationship between Accumulated Strain and HWTD Rut Depth

To validate the relationships proposed in Section 3.3, the PRESS procedure was performed and a sample calculation is included for better understanding of the procedure. The data used in this example is for HWTD test results at the center of specimen for Type D mix and repeated creep tests performed at 52 °C on RTFO aged binder. The measured accumulated strain and HWTD rut depths are shown in Table 4.5. In addition, the regression coefficients obtained for the Type D mix are shown in the last row of the table.

The accumulated strain and rut depth data for W76 are removed and linear regression is performed for the remainder of the data set (9 points). The results of linear regression are shown in Table 4.6. As expected, R^2 value reduced from 0.8296 to 0.8172 while the slope and intercept values changed minimally. The slope and intercept values were then used to estimate rut depth for W76 asphalt, which is reported as 2.7678 in Table 4.6. The $\bar{Y}$ for the data set also changed from 7.04 to 7.52 when the first data point is removed. This procedure is repeated by removing the next data point in turn, replacing the previously removed data point as the analysis progressed. Therefore, the data for W76 is included and W70 data is removed in the next step and so forth. To estimate PRESS R^2, Equation 4.1 is then used for comparison.

The linear regression coefficients obtained from the PRESS procedure and complete data set are included in Tables 4.7 through 4.12. The first set of tables (4.7 though 4.9) show test results for unaged binders while tables 4.10 through 4.12 show data for aged binders. Also found in the tables are the calculated Standard Error values for the data sets.

Table 4.5 Data from a 52 °C DSR Test Performed on all Binders and Rut Depth from a HWTD Test Performed on Type D Material

Mix Type	Binder Type	DSR Accumulated Strain,%	Center of Specimen Deformation, mm	
			Measured	Estimated
Type D	W 76	0.4946	2.7	2.75565
	W 70	0.3565	2.9	2.392488
	W 64	2.427	4	7.837282
	V 64	3.504	14.2	10.66947
	V 70	0.6104	2.3	3.060169
	V 76	1.828	4.7	6.262092
	U 67	1.474	9.2	5.331178
	U 76	0.5449	2.5	2.887924
	B 64	6.297	17.8	18.01422
	B 70	3.702	10.1	11.19015
	Y bar Average		7.04	
Slope = 2.6297; Intercept = 1.4550; R^2 = 0.8296				

Table 4.6 Data from a 52 °C DSR Test Performed on all Remaining Binders and Rut Depth from a HWTD Test Performed on Type D Material

Mix Type	Binder Type	DSR Accumulated Strain,%	Center of Specimen Deformation, mm	
			Measured	Estimated
Type D	W 76	-0.4946		2.767868
	W 70	0.3565	2.9	
	W 64	2.427	4	
	V 64	3.504	14.2	
	V 70	0.6104	2.3	
	V 76	1.828	4.7	
	U 67	1.474	9.2	
	U 76	0.5449	2.5	
	B 64	6.297	17.8	
	B 70	3.702	10.1	
	Y bar Average		7.52	
Slope = 2.6263; Intercept = 1.4689; R^2 = 0.8172				

Table 4.7 PRESS and Graphical R^2 Values, Slope, Intercept and Standard Error for CMHB-C and Type D Mixes with Unaged Binder at 52 °C

	Center of Specimen				Center of Slab				Maximum Deformation			
Type CMHB-C	Slope	1.6177	Standard Error	2.27	Slope	1.8183	Standard Error	3.20	Slope	1.7055	Standard Error	3.12
	Intercept	4.4971	Graphically R^2	0.7055	Intercept	4.6007	Graphically R^2	0.6045	Intercept	5.7254	Graphically R^2 =	0.5848
	PRESS Procedure R^2 =0.5355				PRESS Procedure R^2 =0.5171				PRESS Procedure R^2 =0.4064			
Type D	Slope	2.4104	Standard Error	2.62	Slope	2.2880	Standard Error	4.11	Slope	2.3910	Standard Error	4.15
	Intercept	2.8785	Graphically R^2	0.7994	Intercept	3.2297	Graphically R^2	0.5942	Intercept	4.0019	Graphically R^2 =	0.6105
	PRESS Procedure R^2 =0.3715				PRESS Procedure R^2 =0.1635				PRESS Procedure R^2 =0.0277			
Combined	Slope	2.0140	Standard Error	2.46	Slope	2.0532	Standard Error	3.52	Slope	2.4083	Standard Error	3.55
	Intercept	3.6878	Graphically R^2	0.7385	Intercept	3.9152	Graphically R^2	0.5887	Intercept	4.8636	Graphically R^2 =	0.5837
	PRESS Procedure R^2 =0.7013				PRESS Procedure R^2 =0.5679				PRESS Procedure R^2 =0.5500			

Table 4.8 PRESS and Graphical R^2 Values, Slope, Intercept and Standard Error for CMHB-C and Type D Mixes with Unaged Binder at 64 °C

	Center of Specimen				Center of Slab				Maximum Deformation			
Type CMHB-C	Slope	0.3120	Standard Error	2.15	Slope	0.3773	Standard Error	2.64	Slope	0.3540	Standard Error	2.62
	Intercept	4.4397	Graphically R^2	0.7365	Intercept	4.2932	Graphically R^2	0.7305	Intercept	5.4358	Graphically R^2 =	0.7072
	PRESS Procedure R^2 =0.6632				PRESS Procedure R^2 =0.5984				PRESS Procedure R^2 =0.4882			
Type D	Slope	0.4707	Standard Error	2.23	Slope	0.4841	Standard Error	3.25	Slope	0.4857	Standard Error	3.60
	Intercept	2.7404	Graphically R^2	0.8554	Intercept	2.7579	Graphically R^2	0.7464	Intercept	3.6927	Graphically R^2 =	0.7071
	PRESS Procedure R^2 =0.6185				PRESS Procedure R^2 =0.2345				PRESS Procedure R^2 =0.1338			
Combined	Slope	0.3913	Standard Error	2.24	Slope	0.4307	Standard Error	2.87	Slope	0.4199	Standard Error	3.07
	Intercept	3.5900	Graphically R^2	0.7825	Intercept	3.5255	Graphically R^2	0.7270	Intercept	4.5643	Graphically R^2 =	0.6883
	PRESS Procedure R^2 =0.7509				PRESS Procedure R^2 =0.6942				PRESS Procedure R^2 =0.6464			

Table 4.9 PRESS and Graphical R^2 Values, Slope, Intercept and Standard Error for CMHB-C and Type D Mixes with Unaged Binder at 76 °C

	Center of Specimen				Center of Slab				Maximum Deformation			
Type CMHB-C	Slope	0.0938	Standard Error	2.35	Slope	0.1117	Standard Error	2.98	Slope	0.1054	Standard Error	2.94
	Intercept	3.6438	Graphically R^2	0.6844	Intercept	3.4014	Graphically R^2	0.6572	Intercept	4.6085	Graphically R^2 =	0.6332
	PRESS Procedure R^2 =0.4018				PRESS Procedure R^2 =0.5949				PRESS Procedure R^2 =0.5808			
Type D	Slope	0.1395	Standard Error	2.80	Slope	0.1528	Standard Error	3.14	Slope	0.1521	Standard Error	2.57
	Intercept	1.6189	Graphically R^2	0.7721	Intercept	1.2447	Graphically R^2	0.7635	Intercept	2.2184	Graphically R^2 =	0.7126
	PRESS Procedure R^2 =0.7331				PRESS Procedure R^2 =0.7481				PRESS Procedure R^2 =0.6979			
Combined	Slope	0.1167	Standard Error	2.57	Slope	0.1322	Standard Error	2.99	Slope	0.1283	Standard Error	3.20
	Intercept	2.6340	Graphically R^2	0.7145	Intercept	2.3230	Graphically R^2	0.7037	Intercept	3.4135	Graphically R^2 =	0.6605
	PRESS Procedure R^2 =0.6815				PRESS Procedure R^2 =0.6886				PRESS Procedure R^2 =0.6448			

Table 4.10 PRESS and Graphical R^2 Values, Slope, Intercept and Standard Error for CMHB-C and Type D Mixes with RTFO Aged Binder at 52 °C

	Center of Specimen				Center of Slab				Maximum Deformation			
Type CMHB-C	Slope	1.8928	Standard Error	1.66	Slope	2.1084	Standard Error	2.74	Slope	1.9482	Standard Error	2.80
	Intercept	3.2700	Graphically R^2	0.8422	Intercept	3.2620	Graphically R^2	0.7087	Intercept	4.5322	Graphically R^2 =	0.6654
	PRESS Procedure R^2 =0.7914								PRESS Procedure R^2 =0.6898			
Type D	Slope	2.6297	Standard Error	2.42	Slope	2.4638	Standard Error	4.08	Slope	2.6419	Standard Error	3.94
	Intercept	1.4550	Graphically R^2	0.8296	Intercept	1.9474	Graphically R^2	0.6008	Intercept	2.5190	Graphically R^2 =	0.6499
	PRESS Procedure R^2 =0.8172								PRESS Procedure R^2 =0.5690			
Combined	Slope	2.2612	Standard Error	2.08	Slope	2.2861	Standard Error	3.01	Slope	2.2951	Standard Error	3.30
	Intercept	2.3625	Graphically R^2	0.8117	Intercept	2.6047	Graphically R^2	0.6364	Intercept	2.5256	Graphically R^2 =	0.6389
	PRESS Procedure R^2 =0.7980								PRESS Procedure R^2 =0.6246			

Table 4.11 PRESS and Graphical R^2 Values, Slope, Intercept and Standard Error for CMHB-C and Type D Mixes with RTFO Aged Binder at 64 °C

	Center of Specimen				Center of Slab				Maximum Deformation			
Type CMHB-C	Slope	0.3020	Standard Error	1.94	Slope	0.3314	Standard Error	3.05	Slope	0.3044	Standard Error	3.09
	Intercept	3.8384	Graphically R^2	0.7847	Intercept	3.9519	Graphically R^2	0.6410	Intercept	5.1907	Graphically R^2 =	0.5946
	PRESS Procedure R^2 =0.7608				PRESS Procedure R^2 =0.6137				PRESS Procedure R^2 =0.5680			
Type D	Slope	0.4286	Standard Error	2.58	Slope	0.4134	Standard Error	3.98	Slope	0.4319	Standard Error	4.02
	Intercept	2.1415	Graphically R^2	0.8066	Intercept	2.4553	Graphically R^2	0.6190	Intercept	3.1937	Graphically R^2 =	0.6357
	PRESS Procedure R^2 =0.7901				PRESS Procedure R^2 =0.5812				PRESS Procedure R^2 =0.5710			
Combined	Slope	0.3653	Standard Error	2.28	Slope	0.3724	Standard Error	3.39	Slope	0.3682	Standard Error	3.47
	Intercept	2.9900	Graphically R^2	0.7753	Intercept	3.2036	Graphically R^2	0.6182	Intercept	4.1922	Graphically R^2 =	0.6018
	PRESS Procedure R^2 =0.7584				PRESS Procedure R^2 =0.6060				PRESS Procedure R^2 =0.5867			

Table 4.12 PRESS and Graphical R^2 Values, Slope, Intercept and Standard Error for CMHB-C and Type D Mixes with RTFO Aged Binder at 76 °C

	Center of Specimen				Center of Slab				Maximum Deformation			
Type CMHB-C	Slope	0.0677	Standard Error	1.98	Slope	0.0758	Standard Error	2.97	Slope	0.0698	Standard Error	3.01
	Intercept	3.4231	Graphically R^2	0.7757	Intercept	3.4131	Graphically R^2	0.6587	Intercept	4.6836	Graphically R^2 =	0.6147
	PRESS Procedure R^2 =0.7470				PRESS Procedure R^2 =0.6133				PRESS Procedure R^2 =0.5751			
Type D	Slope	0.0979	Standard Error	2.43	Slope	0.0963	Standard Error	3.76	Slope	0.1012	Standard Error	3.72
	Intercept	1.4487	Graphically R^2	0.8277	Intercept	1.6787	Graphically R^2	0.6610	Intercept	2.3506	Graphically R^2 =	0.6863
	PRESS Procedure R^2 =0.8052				PRESS Procedure R^2 =0.6307				PRESS Procedure R^2 =0.6628			
Combined	Slope	0.0828	Standard Error	2.23	Slope	0.0861	Standard Error	3.25	Slope	0.0855	Standard Error	3.30
	Intercept	2.4359	Graphically R^2	0.7835	Intercept	2.5459	Graphically R^2	0.6489	Intercept	3.5171	Graphically R^2 =	0.6382
	PRESS Procedure R^2 =0.7645				PRESS Procedure R^2 =0.6341				PRESS Procedure R^2 =0.6248			

The PRESS procedure further validates the previous assessment that the correlation levels are lower between the unaged accumulated strain and the HWTD rut depth. The R^2 values obtained from the PRESS procedure are lower than the R^2 values obtained from the complete data set, as expected. In several instances it can be seen that the PRESS R^2 value is significantly less than that of the value found using the complete data set. For example, R^2 value of only 0.03 in comparison to 0.61 was observed for Type D mix at 52 °C (maximum deformation) when the PRESS procedure was used. At 52 °C CMHB-C was exceptionally far off at all three temperatures, while Type D was close at 76 °C but exceedingly off at the other two temperatures. The combined CMHB-C and Type D analysis provided the closest correlation for the unaged binder with the PRESS being only slightly less than the complete data set at all three temperatures.

The Standard Error calculation ranged from 2.3 to 4.2 with the least amount of error occurring at the center of specimen for CMHB-C and the greatest amount of error occurring when correlating the maximum deformation for Type D. Thus, it can be stated that correlating the accumulated strain of unaged binder to the rut depth does not yield a sufficiently strong relationship to make an accurate prediction of rut depth based on binder testing.

Tables 4.10 to 4.12 compare the R^2 values obtained from both the complete set and the PRESS Procedure of the RTFO aged binders tested at all three temperatures for both mix designs. The results show similar trends of reduction in R^2 when the PRESS procedure was used. However, the drop in PRESS was not significant in comparison to unaged binder tests, indicating that better correlation between accumulated stain and rut depth exists when the binder is short term aged. In addition, the R^2 values remained higher when rut depth (measured at the center of the specimen) is compared to accumulated strain measured at 52 °C, indicating that the accumulated strain tests needed to be performed at 52 °C because it is closest to the HWTD test temperature of 50 °C.

As in the previous tables, the standard error of prediction is given for each data set. Similar trends were observed, i.e., for all three temperatures the center of specimen exhibited the least amount of error with CMHB-C correlating better than Type D and the temperature of 52 °C having the best correlation. Therefore, the center of specimen relationships of Type D and CMHB-C proposed in section 3.3 needs to be further evaluated with large pool of data set.

4.3.4.2 Validation of Relationship between $G^*/\sin\delta$ and HWTD Rut Depth

In Table 4.13, the R^2 values, standard errors and PRESS validation are summarized for two mix types using $G^*/\sin\delta$ of aged binder and all three areas of deformation of HMAC. There seems to be a reasonable correlation between the HWTD and $G^*/\sin\delta$ for the CMHB-C mix at the center of specimen, with PRESS values nearly the same in some instances, but the standard error is high in all cases for all the temperatures and mix types indicating that the correlation does not explain relationship between the two parameters very well. In addition, the

HWTD tests are performed at 50 °C; therefore, it is expected that the relationship should be better at 52°C.

By performing the PRESS procedure on the set of data, we find that the relationship between G*/sinδ and HWTD rut depth is valid at the higher temperatures and loses validity as the temperature decreases. Overall, the relationship between G*/sinδ and HWTD seems to be a weak relationship and needs further evaluation.

Compiling the results from HWTD rut depth (Type D and CMHB-C), DSR accumulated strain and DSR G*/sinδ, a general assessment of the rutting potential of the binders was completed. The performance exhibited by the material in each test was ranked and the ranking provided by each test type is shown in Table 4.14. Overall, the validation results suggest that the proposed relationships are valid and can be used to predict rutting potential of asphalt binders. The test results also suggest that the modifiers improve performance but whether or not a specific modifier is better than another cannot be identified.

Table 4.13 R^2 and Standard Error Values for HWTD vs. G*/sinδ

Mix Type	Statistical Parameter	Center of Specimen			Center of Slab			Maximum		
		Binder Test Temperature, °C			Binder Test Temperature, °C			Binder Test Temperature, °C		
		52	64	76	52	64	76	52	64	76
Type D	PRESS	0.1472	0.5947	0.6649	0.0107	0.2905	0.4563	0.2181	0.4132	0.4434
	R^2	0.3739	0.5907	0.7100	0.1924	0.3785	0.5406	0.2750	0.4688	0.6214
	Standard Error	12432.2	3193.6	1068.6	14060.4	3800.3	1221.9	13519.9	3565.8	1127.7
CMHB-C	PRESS	0.654	0.7507	0.7349	0.4316	0.6586	0.6871	0.3504	0.6181	0.6314
	R^2	0.5860	0.6968	0.8275	0.5264	0.5959	0.6933	0.5226	0.6186	0.7412
	Standard Error	9486.0	2374.2	731.8	10047.9	2741.8	938.0	10737.1	2824.3	887.8

Table 4.144 Ranking of Overall Performance of Binder in DSR and HWTD Testing

Asphalt Type	HWTD Ranking		Asphalt Binder Ranking	
	Center of Specimen Deformation, mm		Acc Strain (%) at 52 °C	G*/sinδ (kPa) at 52 °C
	Type D	CMHB-C		
Wright Asphalt 64-22	5 (4.0)	6 (8.0)	7 (2.43)	7 (3.66e2)
Wright Asphalt 70-22 (3.5% SBS)	4 (2.9)	2 (3.4)	1 (0.36)	1 (1.21e3)
Wright Asphalt 76-22 (SBS + TR)	3 (2.5)	4 (4.1)	2 (0.49)	4 (9.22e2)
Valero Armor 64-22	9 (14.2)	8 (9.3)	8 (3.50)	8 (2.91e2)
Valero 76-22 (3.5% Elvaloy)	1 (2.3)	1 (2.6	4 (0.61)	3 (9.65e2)
Valero 70-22 (2% Elvaloy)	6 (4.7)	9 (10.6)	6 (1.83)	6 (3.74e2)
Ultra Base 67-22	7 (9.2)	5 (7.2)	5 (1.47)	5 (4.90e2)
Ultra 76-22 (3.5% SBR)	2 (2.5)	3 (3.5)	3 (0.54)	2 (1.09e3)
BASF 64-22 (0% SBR)	10 (17.8)	10 (15.0)	10 (6.30)	10 (1.12e2)
BASF 70-22 (2% SBR)	8 (10.1)	7 (9.2)	9 (3.70)	9 (1.80e2)

4.4 Elastic Recovery Test Results

The elastic recovery tests were performed on three specimens and the test results are summarized in Table 4.15. Although Tex-539-C suggests performing tests on unaged binders, the tests were also performed on RTFO aged binders and results of the aged binder tests are included. The test results suggest that the aged binders exhibit lower elastic recovery in comparison to unaged binders. The test results also suggest that the test is repeatable as the coefficient of variance is less than 5% in most cases.

The unaged asphalt binder test results suggest that all of the binders are acceptable. The aged binder test results suggest that all of the binders are acceptable except U 76 SBR (Ultrapave). Since the U 76 SBR fails the requirement by only 0.7%, which is within the range of test error, it may be acceptable. In addition, HWTD test results suggested that it passes the Tex-242-F criterion of 12.5 mm. This confirms the notion of SBR modified asphalt producers that the SBR does not meet the elastic recovery tests but performs well in the field. Overall, the test results clearly suggest that the Tex-539-C can identify presence of modifier because elastic recovery jumped from 30% to 50% in the presence of modifier.

The data is also graphically presented in Figure 4.29. The results suggest that in most cases RTFO aged binder show lower elastic recovery compared to unaged binders. Since the aged binder is used in the field, it would be appropriate to perform tests on aged specimens.

Table 4.15 Elastic Recovery Test Results

Binder Type	TxDOT Spec.	Unaged			Aged		
		Elastic Recovery, %	S.D., %	COV, %	Elastic Recovery, %	S.D., %	COV, %
Wright Asphalt 64-22	--	29.7	1.53	5.15	31.3	2.08	6.64
Wright Asphalt 70-22 (3.5% SBS)	30%	61.0	1.00	1.64	52.3	0.58	1.10
Wright Asphalt 76-22 (SBS + TR)	50%	78.3	0.58	0.74	64.0	1.00	1.56
Valero Armor 64-22	--	31.0	1.00	3.23	28.0	1.73	6.19
Valero 76-22 (3.5% Elvaloy)	50%	52.7	0.58	1.10	**49.3**	0.58	1.17
Valero 70-22 (2% Elvaloy)	30%	25.7	0.58	2.25	25.7	0.58	2.25
Ultra Base 67-22	--	54.7	0.58	1.06	55.3	1.15	2.09
Ultra 76-22 (3.5% SBR)	50%	54.7	0.58	1.06	57.7	0.58	1.00
BASF 64-22 (0% SBR)	--	24.7	0.58	2.34	29.3	0.58	1.97
BASF 70-22 (2% SBR)	--	49.7	0.58	1.16	47.3	0.58	1.22

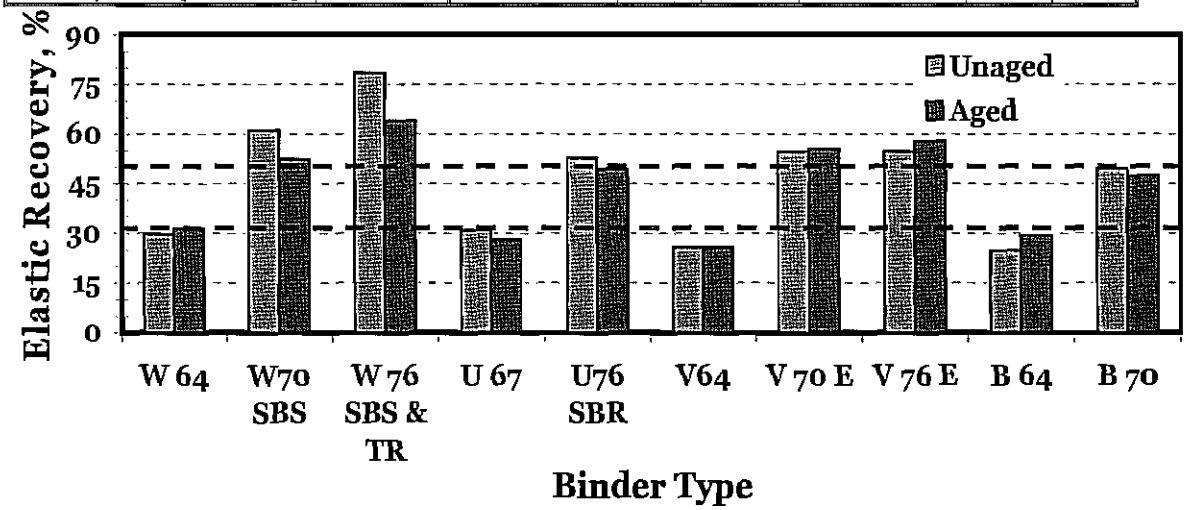

Figure 4.29 Graphical Representation of Elastic Recovery Test Results

For comparison with the rut depth predicted by HWTD tests, the results from the two devices are presented in Figure 4.30. The results suggest there is no relationship between elastic recovery and rut depth. The data only suggest that more than 45% elastic recovery indicates presence of modifier. The test results suggest that no correlation exists between HWTD and Tex-539-C. Therefore, Tex-539-C is not suitable for predicting rutting of HMAC.

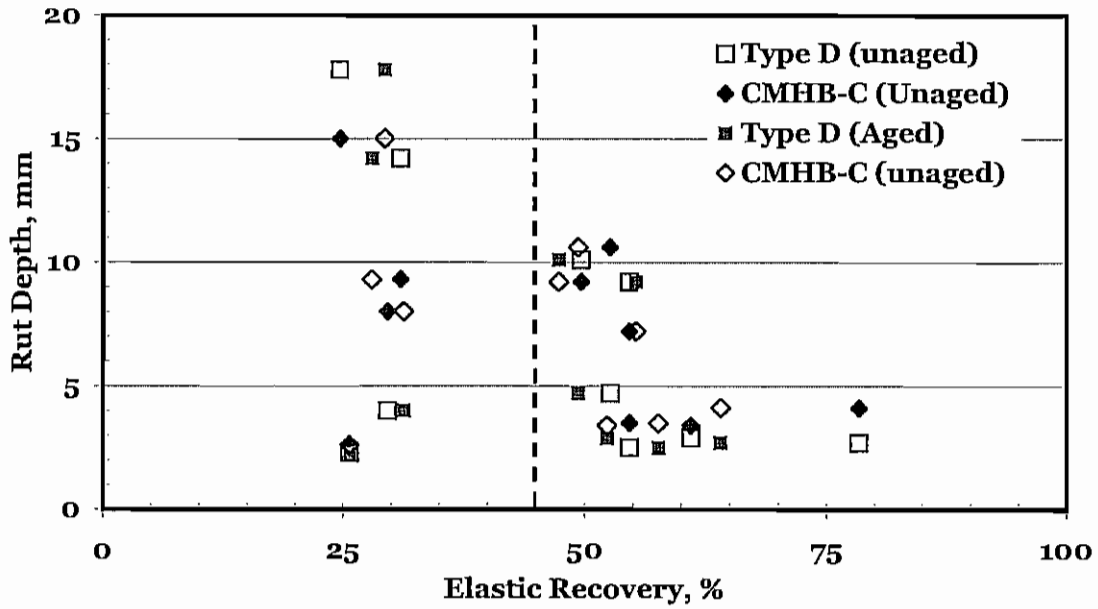

Figure 4.30 HWTD Rut Depth vs. Elastic Recovery Results

Based on the test results presented, it can be concluded that Tex-539-C can identify the presence of modifiers. The results suggest that Tex-539-C be modified to perform tests on RTFO aged binders. In addition, it is not suitable for identifying rut potential of HMAC.

4.5 Cracking Potential of HMAC from Binder Tests

As mentioned earlier, the flexural beam fatigue tests were performed on CMHB-C and Type D mixes and the test results have been included in Research Report No. 0-4824-2 (Rajpal et al., 2007). The summarized test results have been included in Tables 4.16 and 4.17 for the CMHB-C and Type D mixture, respectively. The test results are shown for tests performed at 500 με. It should be noted that the results have been obtained using the current failure criterion as per AASHTO specifications. The test results suggest that the modified binders exhibit higher fatigue lives in comparison to base binders. The fatigue lives of Type D mixes are generally longer than those corresponding to the CMHB-C mixes, indicating that Type D has a higher resistance to fracture and fatigue.

The tables also include G*sinδ (indicator of fatigue resistance) values of PAV aged binders tested at 31 °C and 10 rad/sec frequency. The test results from Valero Armor asphalt are not included because they were not tested. The test results suggest that the G*sinδ value increased when modifier was added for Wright Asphalt while opposite trend was observed for Ultrapave binder. This suggests that the modifier is reacting with base binder and reducing the stiffness at the

tested temperature. To obtain relationship between G*sinδ and fatigue life, the data from the two tests is included in Figure 4.31. The data shows that the G*sinδ value of base binder (supplied by Ultrapave) is higher but the fatigue life is similar to the other base binder types suggesting that it could be an outlier. If the Ultrapave base binder data is eliminated, a very good exponential correlation exists between G*sinδ and fatigue life. The R^2 value for both mix types is more than 0.90 indicating that it is feasible to estimate fatigue life from G*sinδ of binder; however, more research is needed to validate this relationship.

Table 4.15 Results of the Fatigue Test for CMHB-C Mixes

Manufacturer	PG Grade	Modifier Type	G*sinδ, kPa	Average No. of Cycles
Wright Asphalt	PG64-22	Unmodified	1,978.9	49,395
	70-22	3.5% SBS	2,184.8	230,585
	76-22	SBS+TR	2,374.8	401,210
Ultrapave	67-22	Unmodified	3,086	119,510
	76-22	3.5% SBR	2,585	1,185,550
Valero Asphalt	64-22	Unmodified	NT	136,240
	76-22	3.5% Elvaloy	NT	1,145,505

Table 4.16 Results of the Fatigue Test for Type D Mixes

Manufacturer	PG Grade	Modifier Type	G*sinδ, kPa	Average No. of Cycles
Wright Asphalt	PG64-22	Unmodified	1,978.9	132,905
	70-22	3.5% SBS	2,184.8	653,940
	76-22	SBS+TR	2,374.8	937,340
Ultrapave	67-22	Unmodified	3,086	252,745
	76-22	3.5% SBR	2,585	2,740,495
Valero Asphalt	64-22	Unmodified	NT	470,555
	76-22	3.5% Elvaloy	NT	2,423,715

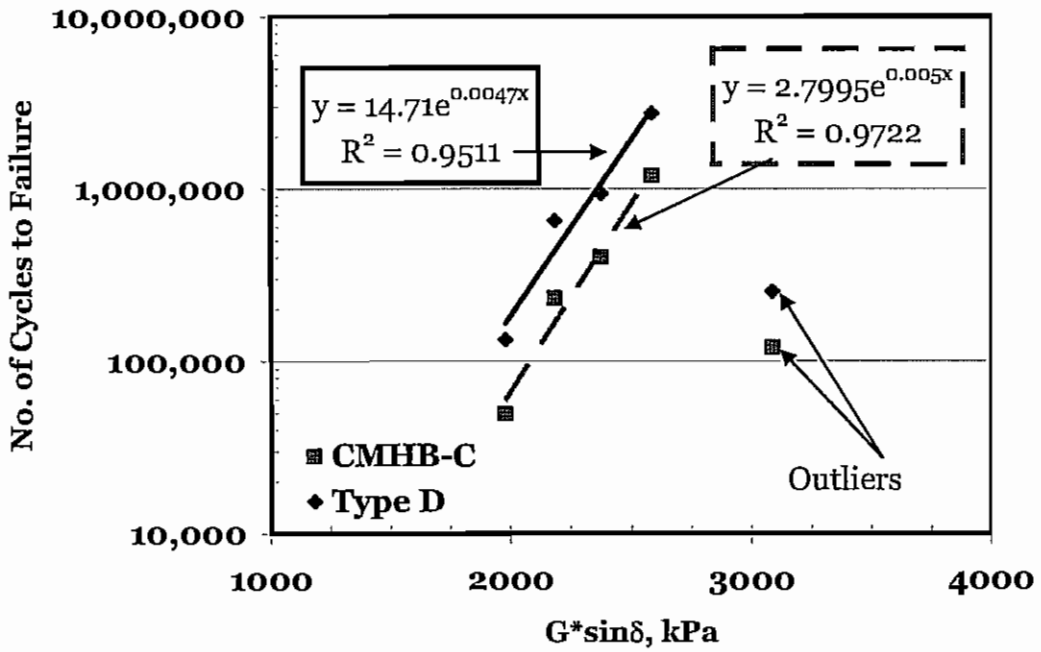

Figure 4.31 Relationship between Fatigue Beam and G*sinδ

CHAPTER 5 CONCLUSION AND RECOMMENDATIONS

5.1 CONCLUSIONS

The evaluation of the Tex-539-C test suggests that the test can detect the presence of modifiers. The results suggest that the Tex-539-C be modified to perform tests on RTFO aged binders and the specifications can be modified accordingly. However, the test is not suitable for predicting the rutting potential of HMAC.

The performance of asphalt binders, base and modified, was evaluated in order to form a relationship between the HWTD rut deformation and the DSR accumulated strain. It was determined with strong certainty (R^2 from 0.82 to 0.84) that the rut of a Type D or CMHB-C mix at the center of the specimen can be predicted by substituting the accumulated strain of the RTFO aged binder into the equations $y = 2.6297x + 1.455$ and $y = 1.8928x + 3.27$, respectively. For a slightly lower reliability (R^2 of 0.81) the accumulated strain can be input into the combined equation $y = 2.2612x + 2.3625$.

A general assessment can be made that if the accumulated strain of the RTFO aged binder at 52 °C is less than 1%, a modifier is present. If this binder is used with a Type D or CMHB-C mix design, a minimal rut depth (< 5mm) can be expected in HMAC specimens provided HMAC meets specified volumetric. Any RTFO aged binder tested at 52 °C with an accumulated strain greater than 2.5% is considered to be an unmodified binder, PG 64, or a binder containing a poor modifier likely to have weak rut resistance. If this binder is used with a Type D or CMHB-C mix design, high deformation (> 10mm) of HMAC should be anticipated.

The $G^*/\sin\delta$ value at 1.59 Hz (10 rad/sec.) is not able to detect the presence of modifier and does not correlate well with the HWTD rut depth. However, the $G^*/\sin\delta$ value at 0.5 Hz or lower frequency and at the temperature higher than PG grade can identify presence of modifier. In addition, the aged $G^*/\sin\delta$ values at 76 °C correlate well with the HWTD rut depth. However, more tests are needed before definite conclusion can be drawn.

The cracking resistance of binder increases with the presence of modifier and the limited data set suggests that the fatigue resistance ($G^*\sin\delta$) of the asphalt binder can be used to estimate the fatigue resistance of mixes. However, more work is needed before definite conclusions can be drawn.

5.2 RECOMMENDATIONS

- Further testing with more binders and different mix types to form different correlations.
- Testing at different shear stresses to determine if a stronger correlation exists at other stresses levels.

REFERENCES

1. Anderson, D. A., Y. M. Le Hir, J. P. Planche, and D. Martin. (2002) "Zero Shear Viscosity of Asphalt Binders." Transportation Research Record 1810, Transportation Research Board, Washington D. C., pp. 54-62.
2. Aschenbrener, T. (1995) "Evaluation of the Hamburg Wheel-Tracking Device to Predict Moisture Damage in Hot-Mix Asphalt." Transportation Research Record 1492, Transportation Research Board, Washington, D.C., pp. 193-201.
3. Bahia, H. U., D. I. Hanson, M. Zeng, H. Zhai, et. al. (2001) "Characterization of Modified Asphalt Binders in Superpave Mix Design." NCHRP Report 459, Transportation Research Board, Washington D.C.
4. Button, Joe W., (2004) "New Simple Performance Tests of Asphalt Mixes." No. E-C068, ISSN 0097-8515, Transportation Research Board, Washington D.C.
5. Carswell, J., M. J. Claxton, and P. J. Green. "Dynamic Shear Rheometers." BP Oil International.
6. Dongre, R., J. D'Angelo, (2003) "Refinement of Superpave High-Temperature Binder Specification Based on Pavement Performance in the Accelerated Loading Facility." Transportation Research Board 1829, Transportation Research Board, Washington D. C., pp. 39-46.
7. Gina, H. (2006), "Estimation of Hot Mix Asphalt Concrete Rutting Potential from Asphalt Binder Tests," University of Texas at El Paso, El Paso, Texas.
8. Herh, Peter K. W., Steven M. Cole, Kaj Hendınan, and Bruce K. S. Rudolph. (1997) "Dynamic Shear Rheometers Pave The Way for Quality Asphalt Binders." Viscotech DSR.
9. King, Gayle, Helen King, R. D. Pavlovich, Amy L. Epps and Prithvi Kandhal. (1999) "Additives in Asphalt." Journal of Association of Asphalt Paving Technologists, Vol. 68A.
10. Kraier, K. B., D. L. Wolfe, and J. A. Epps, "Field Trials of Plastic and Latex Modified Asphalt Concrete." Transportation Research Board 1171, Transportation Research Board, Washington, D.C.
11. Maher, Ali, "Investigation into Modified Asphalt Binders for Improved Pavement Performance." Project 80-RU908 Center for Advanced Infrastructure & Transportation (CAIT) Rutgers, The State University of New Jersey.
12. Marasteanu, Mihai O., T. Clyne, J. McGraw, et. al. (2005) "High-Temperature Rheological Properties of Asphalt Binders." ISSN 0361-1981. Annual Meeting of Transportation Research Board, Washington D.C.
13. Pagen, C. A. (1963), "*An Analysis of the Themorheological Response of Bituminous Concrete,*" Master of Science Thesis, The Ohio State University, pp. 26-33

14. "Pavement Selection for City Streets." Texas Asphalt Pavement Association, (TxAPA), 2005.
15. Rajpal, S., Zea, M., Tandon, V., Smit, A., and Prozzi, J. (2007), "Performance Evaluation of HMA Consisting of Modified Asphalt Binder," Report No. FHWA/TX-07/0-4824-2, Center for Transportation Infrastructure Systems, The University of Texas at El Paso, El Paso, Texas.
16. Rajpal, S. (2005) "Rutting Potential of Polymer Modified Hot Mix Asphalt Concrete Mixes." University of Texas at El Paso, El Paso, Texas.
17. Romero, P., K. Stuart. (1998) "Evaluating Accelerated Rut Testers." FHWA July/August Vol. 62 No. 1.
18. Roque, Reynaldo, B. Birgisson, C. Drakos, and G. Sholar. (December 2004) "Guidelines for Use of Modified Binders." Florida Department of Transportation (FDOT) Report Number 4910-4504-964-12.
19. Sagi, S. V. (2004) "The Impact of Acceptance Criterion on HMAC Moisture Susceptibility." University of Texas at El Paso, El Paso, Texas.
20. Seeds, Stephen B., N.C. Jackson, J. Ziegler. (1998) "Techniques for Pavement Rehabilitation." National Highway Institute (NHI).
21. Smit, A., Prozzi, J., and Tandon, V. (2004) "Project Survey for Usage of Hot Mix Asphalt Concrete," Technical Memorandum Project 0-4824-1, Center for Transportation Research, The University of Texas at Austin, Austin, Texas.
22. Tandon, V. (1994) "Streamlining, Calibration, and Validation of the Preliminary SHRP Thermal Cracking Performance Prediction Model."
23. Youtcheff, Jack S., and Jones, D. (1994) "Guideline for Asphalt Refiners and Suppliers," Strategic Highway Research Program, SHRP-A-686, Washington, D.C.